Available online at www.sciencedirect.com
SCIENCE DIRECT®
Nuclear Physics B 750 [FS] (2006) 142–178
NUCLEAR PHYSICS B

Some formal results for the valence bond basis

K.S.D. Beach *, Anders W. Sandvik

Department of Physics, Boston University, 590 Commonwealth Avenue, Boston, MA 02215, USA

Received 4 May 2006; accepted 17 May 2006

Available online 21 June 2006

Abstract

In a system with an even number of SU(2) spins, there is an overcomplete set of states—consisting of all possible pairings of the spins into valence bonds—that spans the $S = 0$ Hilbert subspace. Operator expectation values in this basis are related to the properties of the closed loops that are formed by the overlap of valence bond states. We construct a generating function for spin correlation functions of arbitrary order and show that all nonvanishing contributions arise from configurations that are topologically irreducible. We derive explicit formulas for the correlation functions at second, fourth, and sixth order. We then extend the valence bond basis to include triplet bonds and discuss how to compute properties that are related to operators acting outside the singlet sector. These results are relevant to analytical calculations and to numerical valence bond simulations using quantum Monte Carlo, variational wavefunctions, or exact diagonalization.

PACS: 03.65.Ca; 74.20.Mn; 75.10.Jm; 75.50.Ee

Keywords: Valence bonds; Quantum spin systems; Heisenberg model

1. Introduction

The traditional way to represent the quantum states of a system of $S = 1/2$ spins is to introduce a basis of S^z eigenstates. Each state corresponds to a particular assignment of "up" or "down" to each spin in the lattice. This basis is complete and orthonormal. Another useful basis, dating back to Rumer and Pauling in the 1930s [1,2], is the so-called *valence bond basis*, in which the states of the system are represented by partitions of the spins into pairs forming singlets. A valence

* Corresponding author.
E-mail address: ksdb@bu.edu (K.S.D. Beach).

0550-3213/$ – see front matter
doi:10.1016/j.nuclphysb.2006.05.032

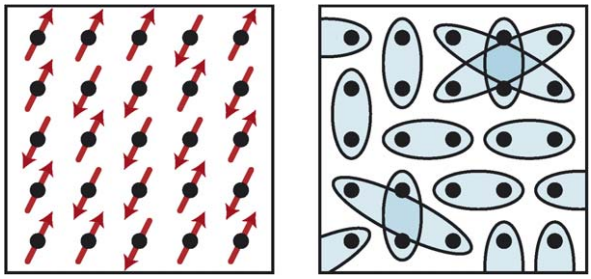

Fig. 1. The low-energy singlet sector of quantum antiferromagnets can be described in either the S^z or valence bond basis.

bond (VB) state,

$$|v\rangle = \prod_{ij} [i, j], \tag{1}$$

is a product of singlets,

$$[i, j] = \frac{1}{\sqrt{2}}\big(|\uparrow_i \downarrow_j\rangle - |\downarrow_i \uparrow_j\rangle\big), \tag{2}$$

in which each site label appears only once. Pictorially, a VB state can be represented as a system of hard-core dimers, where each lattice site (spin) belongs to exactly one dimer, as illustrated in Fig. 1. The VB basis spans the singlet sector of the Hilbert space, but is massively overcomplete. It is also highly nonorthogonal, having the unusual property that every two states in the basis have nonzero overlap.

The first important work in this basis was the calculation of the ground-state energy per spin of the infinite quantum Heisenberg chain by Hulthén [3] (building on the earlier work of Bethe [4]). Hulthén also determined the eigenvalues and eigenstates of small finite chains of up to ten sites using the subset of "noncrossing" [1] valence bond states (which form a complete basis). Majumdar and Ghosh later performed a similar calculation for the one-dimensional spin chain with nearest- and next-nearest-neighbour interactions [5].

The valence bond basis has a special connection to the paramagnetic states of interacting antiferromagnets. Fazekas and Anderson introduced the resonating valence bond (RVB) picture to describe a possible spin liquid in frustrated magnets [6]. Anderson later proposed that a doped RVB state may describe the cuprate superconductors [7,8]. This suggestion spurred wide interest in the VB description of antiferromagnets and possible exotic ground states that are naturally described in terms of VB states. In particular, VB states have proved useful as variational states, where the variational freedom lies in the distribution of valence bond lengths [9–13] or in a set of projected-BCS coefficients [14–16].

Since valence bond states have total spin invariance built in, they are also a natural choice for exact diagonalization within the low-energy $S = 0$ matrix block. Such calculations have been used to study RVB states with a restriction of the VB basis to include only a subset of states with short dimers [17,18], which should be a good approximation for systems with only short-range spin correlations. A generalization of this procedure—in which the valence bonds are antisymmetrized products of individual atomic eigenstates—has been widely adopted by computational chemists for use in molecular quantum mechanics [19,20].

Variational calculations suggest that the collinear Néel ground state of the d-dimensional ($d > 1$) Heisenberg antiferromagnet is well-described by a superposition of VB configurations

whose distribution of bond lengths exhibits $1/r^p$ powerlaw behaviour, with $p < 5$ in two dimensions [9]. In two dimensions, it is also believed that there are magnetically disordered states with energy very close to that of the ordered ground state [9]. Thus, competing interactions may favour RVB states with short-ranged bonds and no long-range magnetic order [21–23]. They may also favour states with valence bond solid (VBS) order [24,25], in which the translational symmetry is broken but the spin-rotational symmetry remains intact. To date, the only firm confirmation of an RVB state is in simplified quantum dimer models [26], in which only the dimer degrees of freedom are retained and the spin degrees of freedom associated with the dimers are neglected.

In most cases, possible exotic spin states [27–30] simply cannot be studied in detail with unbiased methods such as quantum Monte Carlo (QMC), because of the infamous negative-sign problem. QMC simulations of quantum spin systems have traditionally been carried out in the standard S^z basis. Although the feasibility of a Monte Carlo projection for improving a variational VB state was demonstrated more than fifteen years ago [31], the use of the VB basis in QMC studies has been very limited so far [32]. As it turns out, neither the overcompleteness nor the nonorthogonality of the valence bond basis is an impediment to carrying out QMC simulations in principle. In fact, even without a good variational state as a trial state, the ground state can be completely projected out starting with, e.g., an arbitrarily chosen basis state [33] using importance sampling and a simple local updating scheme. This method delivers performance comparable to the current state of the art for S^z-basis QMC calculations (i.e., stochastic series expansion [34] and world line [35] methods with loop-cluster updates). It was also noted in Ref. [33] that the VB projector method expands the class of models that are sign-problem-free. A host of isotropic SU(2) invariant models with multi-spin interactions (involving four, six, etc., spins) can be studied, which in spite of not being frustrated in the standard sense (an odd number of antiferromagnetic interactions around a closed loop on the lattice) do give rise to a sign problem in standard methods. Thus, VB simulations open new opportunities to study ground state phases and transitions in quantum spin systems.

In addition to these new opportunities for QMC studies in the VB basis, we also believe that there is more to do variationally. There was not much follow-up on the pioneering calculations by Liang, Doucot, and Anderson [9], and with the increase in computer performance since that time, it is now feasible to consider more complex wave-function optimizations [13]. Although frustrated systems also cause sign problems in variational calculations, it may still be possible to extract useful information from them. It may also prove fruitful to study variational VB wave functions for nonfrustrated multi-spin interactions.

In both QMC and variational calculations, one would like to study a wide range of physical observables to characterize the ground state. Overlaps and matrix elements between two VB states $|v\rangle$ and $|v'\rangle$ can be related to the structure of the closed loops that are formed when their corresponding dimer configurations are superimposed. There are two standard results: (i) for a system of $2N$ spins, $\langle v|v'\rangle = \pm 2^{N_\circlearrowleft - N}$ where $N_\circlearrowleft \leqslant N$ is the number of loops. $\langle v|v'\rangle$ is unity when the states $|v\rangle$ and $|v'\rangle$ are identical and $N_\circlearrowleft$ is a maximum; its magnitude is halved each time a bond mismatch reduces the loop count by one [36,37]. (ii) $\langle v|\mathbf{S}_i \cdot \mathbf{S}_j|v'\rangle = \pm\frac{3}{4}\langle v|v'\rangle$ if i and j belong to the same loop and vanishes otherwise [9]. (In each case, the overall sign depends on the convention for assigning directions to the bonds.) We are not aware of expressions for more complicated matrix elements, e.g., those involving more than two spin operators or individual components of the spins. Nor are we aware of expressions for quantities that are associated with triplet excitations or for quantities, such as the spin stiffness, that cannot usually be written in terms of an equal-time correlation function.

The goal of this paper is to provide a formal framework for organizing calculations in the valence bond basis and to present several new formulas relating the loop structure of overlapping valence bond states to a wider range of physical properties of the system. We do this in a formal way, using bond operators equivalent to those first derived by Sachdev and Bhatt [38], which in their usual context are associated with a fixed dimer configuration. Here, we generalize the creation and annihilation operators that describe the states of the two-spin system to the many-spin case, allowing the operators to act between arbitrary pairs of spins. With one additional anticommutator rule, we find that we can use these operators to organize calculations in the overcomplete valence bond basis. As a result, we are then able to address higher-order spin correlations, such as $(\mathbf{S}_i \cdot \mathbf{S}_j)(\mathbf{S}_k \cdot \mathbf{S}_l)$, and demonstrate that their matrix elements are topological in nature, depending not only on the loop membership of the various site labels (as is the case for $\mathbf{S}_i \cdot \mathbf{S}_j$) but also on the overall connectivity of the loops with respect to the (i, j) and (k, l) vertices. We introduce a generating function whose derivatives produce a related class of cumulant function. A diagrammatic expansion elucidates the structure of these functions and greatly simplifies their calculation. We extend the valence bond basis to include triplet as well as singlet bonds in an effort to access the full Hilbert space. This allows us to compute various spin correlation functions component-wise, including two-spin operators of the form $S_i^x S_j^x$ and four-spin operators such as $S_i^x S_j^x S_k^x S_l^x$ and $S_i^x S_j^x S_k^y S_l^y$. We also derive an expression for the singlet-triplet gap and the spin stiffness. These results should be useful in the context of QMC, variational calculations, and in exact diagonalization. Our formalism may also find use in approximate analytical calculations.

The organization of the paper is as follows. In Section 2, we introduce the valence bond operator formalism that is used throughout. The three subsequent sections review how to construct $S = 0$ valence bond states (Section 3), how to describe their evolution under action by a Hamiltonian (Section 4), and how to compute their overlaps (Section 5). In Section 6, we begin to derive formulas for the isotropic spin correlation functions in a somewhat naive way. We reproduce these results in Section 7 using a more sophisticated diagrammatic approach and then carry the calculation to higher order. In Section 8, we develop rules for valence bond states with triplet excitations; these are used in Section 9 to compute correlation functions of components of the staggered magnetization. In Section 10, we discuss the Néel state and how it can be employed as a reference state to compute the singlet–triplet gap (Section 11) and the spin stiffness (Section 12).

2. Valence bond operator formalism

Two SU(2) spins labeled i and j have a total spin $\mathbf{S} = \mathbf{S}_i + \mathbf{S}_j$ satisfying $\frac{1}{2}\mathbf{S}^2 = \frac{3}{4} + \mathbf{S}_i \cdot \mathbf{S}_j$. Thus, the usual Heisenberg interaction can be written as

$$\hat{H}_{ij} = \mathbf{S}_i \cdot \mathbf{S}_j - \frac{1}{4} = \frac{1}{2}\mathbf{S}^2 - 1. \tag{3}$$

The eigenstates of Eq. (3) are states of well-defined total spin, having eigenvalues $\frac{1}{2}S(S+1) - 1$. We enumerate them as follows: one $(S = 0)$ singlet $|0\rangle$ and three $(S = 1)$ triplets $|1\rangle$, $|2\rangle$, $|3\rangle$ with energy $E^\mu = -\delta^{\mu 0}$.

For bookkeeping purposes, it is helpful to introduce a boson representation for the spins,

$$\mathbf{S}_i = \frac{1}{2}\sum_{ss'} b_{is}^\dagger \boldsymbol{\sigma}_{ss'} b_{is'} \quad \text{with} \quad \sum_s b_{is}^\dagger b_{is} = 1 \tag{4}$$

(note the single-occupancy constraint), and to define a valence bond operator

$$\chi_{ij}^{\mu\dagger} = \frac{1}{\sqrt{2}} \sum_{ss'} \tau_{ss'}^{\mu} b_{is}^{\dagger} b_{js'}^{\dagger} \tag{5}$$

that creates eigenstates of $\hat{H}_{ij}$ out of the bosonic vacuum (i.e., $|\mu\rangle = \chi_{ij}^{\mu\dagger}|\text{vac}\rangle$ and $\chi_{ij}^{\mu}|\text{vac}\rangle = 0$). The eigenvalue equation $\hat{H}_{ij}|\mu\rangle = E^{\mu}|\mu\rangle$, now written as

$$\hat{H}_{ij}\chi_{ij}^{\mu\dagger}|\text{vac}\rangle = -\delta^{\mu 0}\chi_{ij}^{0\dagger}|\text{vac}\rangle, \tag{6}$$

determines the unknown coefficients τ^{μ}. One possible solution to Eq. (6) is

$$\tau^{\mu} = \left(\tau^0, \boldsymbol{\tau}\right) = \left(i\sigma^2, i\sigma^3, \mathbb{1}, -i\sigma^1\right), \tag{7}$$

where $\sigma^{\mu} = (\mathbb{1}, \boldsymbol{\sigma})$ denotes the four-vector consisting of the unit matrix and the three Pauli matrices; the resulting states are

$$|\mu\rangle = \chi_{ij}^{\mu\dagger}|\text{vac}\rangle = \begin{cases} \frac{1}{\sqrt{2}}(|\uparrow_i\downarrow_j\rangle - |\downarrow_i\uparrow_j\rangle) & \text{if } \mu = 0, \\ \frac{i}{\sqrt{2}}(|\uparrow_i\uparrow_j\rangle - |\downarrow_i\downarrow_j\rangle) & \text{if } \mu = 1, \\ \frac{1}{\sqrt{2}}(|\uparrow_i\uparrow_j\rangle + |\downarrow_i\downarrow_j\rangle) & \text{if } \mu = 2, \\ \frac{-i}{\sqrt{2}}(|\uparrow_i\downarrow_j\rangle + |\downarrow_i\uparrow_j\rangle) & \text{if } \mu = 3. \end{cases} \tag{8}$$

Other linear combinations of the triplet states are equally valid, but this choice has the advantage that the labels correspond to real physical directions in the standard basis of $\mathbb{R}^3$. This is true in the sense that $S_i^a|0\rangle \sim |a\rangle$ for $a = 1, 2, 3$. The key is that Eq. (7) obeys $\boldsymbol{\sigma}\tau^0 = i\boldsymbol{\tau}$, which implies that $\mathbf{S}_i\chi_{ij}^{0\dagger}|\text{vac}\rangle = (i/2)\boldsymbol{\chi}_{ij}^{\dagger}|\text{vac}\rangle$.

We emphasize that the χ_{ij}^{μ} operators completely describe the $\text{SU}(2)\otimes\text{SU}(2) \simeq \text{SO}(4)$ degrees of freedom of the two-spin system. These operators obey the completeness relation

$$\sum_{\mu} \chi_{ij}^{\mu\dagger}\chi_{ij}^{\mu} = \chi_{ij}^{0\dagger}\chi_{ij}^{0} + \boldsymbol{\chi}_{ij}^{\dagger}\cdot\boldsymbol{\chi}_{ij} = 1, \tag{9}$$

which follows from $\sum_{\mu}\tau_{ss'}^{\mu}\tau_{r'r}^{\mu\dagger} = 2\delta_{sr}\delta_{s'r'}$ and the restriction to one boson per site. The anti-commutation relation

$$\left[\chi_{ij}^{\mu}, \chi_{ij}^{\nu\dagger}\right]|\text{vac}\rangle = \delta^{\mu\nu}|\text{vac}\rangle \tag{10}$$

is inherited from the properties $[b_{is}, b_{js'}^{\dagger}] = \delta_{ij}\delta_{ss'}$ and $b_{is}|\text{vac}\rangle = 0$.

Any valid (i.e., $\sum_s b_{is}^{\dagger}b_{is} = 1$ preserving) operation on one or both of the spins has an SO(4) representation. By construction, the operator equivalence

$$\mathbf{S}_i\cdot\mathbf{S}_j = -\frac{3}{4}\chi_{ij}^{0\dagger}\chi_{ij}^{0} + \frac{1}{4}\boldsymbol{\chi}_{ij}^{\dagger}\cdot\boldsymbol{\chi}_{ij} \tag{11}$$

holds, and elimination of $\boldsymbol{\chi}$ via Eq. (9) yields

$$-\hat{H}_{ij} = \frac{1}{4} - \mathbf{S}_i\cdot\mathbf{S}_j = \chi_{ij}^{0\dagger}\chi_{ij}^{0}. \tag{12}$$

For an arbitrary bilinear operator $\hat{O} = \sum_{\mu\nu} O^{\mu\nu}\chi_{ij}^{\mu\dagger}\chi_{ij}^{\nu}$, two applications of Eq. (10) will coax out the coefficient matrix, $O^{\mu\nu} = \langle\text{vac}|[\chi^{\mu}, [\hat{O}, \chi^{\nu\dagger}]]|\text{vac}\rangle$.

In the case of the spin operators themselves, one finds $(S_i^a)^{\mu\nu} = \frac{1}{2}\operatorname{tr}(\tau^{\mu\dagger}\sigma^a\tau^\nu)$ and $(S_j^a)^{\mu\nu} = \frac{1}{2}\operatorname{tr}(\tau^\nu\sigma^{a*}\tau^{\mu\dagger})$. Evaluation of the traces leads to

$$S_i^a - S_j^a = i\big(\chi_{ij}^{a\dagger}\chi_{ij}^0 - \chi_{ij}^{0\dagger}\chi_{ij}^a\big), \tag{13}$$

$$S_i^a + S_j^a = i\epsilon^{abc}\chi_{ij}^{b\dagger}\chi_{ij}^c. \tag{14}$$

Eqs. (13) and (14) turn out to be very useful, but we should not regard them as the fundamental operator equivalence rules. They seem to suggest that two-spin operations are always quartic in χ_{ij}^μ, which is clearly not true (cf. Eq. (11)).

There is an alternative to computing the coefficient matrix directly. For operators that transform in a known way, we can induce the same transformation in χ_{ij}^μ and equate the corresponding terms. Consider a spin rotation $S^a \to R^{ab}(\theta\mathbf{n})S^b$ of θ radians about the axis $\mathbf{n}$ ($|\mathbf{n}| = 1$). In the boson language, this rotation is equivalent to the unitary transformation $b \to Ub$ with $U(\theta\mathbf{n}) = e^{(i\theta/2)\mathbf{n}\cdot\sigma} = \mathbb{1}\cos(\theta/2) + i\mathbf{n}\cdot\boldsymbol{\sigma}\sin(\theta/2)$. Now suppose that we rotate $\mathbf{S}_i$ and $\mathbf{S}_j$ by two different angles about the same axis: putting $b_i \to U(\theta_i\mathbf{n})b_i$ and $b_j \to U(\theta_j\mathbf{n})b_j$ into Eq. (5), we find that the rotation is equivalent to the valence bond operator transformation

$$\chi_{ij}^0 \to \chi_{ij}^0\cos(\theta_{ij}/2) + \mathbf{n}\cdot\boldsymbol{\chi}_{ij}\sin(\theta_{ij}/2), \tag{15}$$

where $\theta_{ij} = \theta_i - \theta_j$ is the relative rotation angle.

If $\mathbf{n}$ is directed along the 3 axis, the rotation matrix $R^{ab} = \frac{1}{2}\operatorname{tr}U^\dagger\sigma^aU\sigma^b$ has the form

$$R\big(\theta\mathbf{e}^3\big) = \begin{pmatrix} \cos\theta & \sin\theta & 0 \\ -\sin\theta & \cos\theta & 0 \\ 0 & 0 & 0 \end{pmatrix}. \tag{16}$$

Described in terms of raising and lowering operators, the transformation amounts to

$$\begin{aligned} &S^+ \to e^{-i\theta}S^+, \\ &S^- \to e^{i\theta}S^-, \\ &S^3 \to S^3, \end{aligned} \tag{17}$$

and in particular,

$$S_i^+S_j^- + S_i^-S_j^+ \to e^{-i\theta_{ij}}S_i^+S_j^- + e^{i\theta_{ij}}S_i^+S_j^-. \tag{18}$$

Consequently, the isotropic Heisenberg interaction, expanded in powers of θ_{ij}, behaves as

$$\mathbf{S}_i\cdot\mathbf{S}_j \to \mathbf{S}_i\cdot\mathbf{S}_j - \frac{i}{2}\theta_{ij}\big(S_i^+S_j^- - S_i^+S_j^-\big) - \frac{1}{4}\theta_{ij}^2\big(S_i^+S_j^- + S_i^-S_j^+\big). \tag{19}$$

According to Eq. (15), the same transformation applied to the valence bond operators gives

$$\chi_{ij}^{0\dagger}\chi_{ij}^0 \to \chi_{ij}^{0\dagger}\chi_{ij}^0 + \frac{\theta_{ij}}{2}\big(\chi_{ij}^{0\dagger}\chi_{ij}^3 + \chi_{ij}^{3\dagger}\chi_{ij}^0\big) + \frac{\theta_{ij}^2}{4}\big(-\chi_{ij}^{0\dagger}\chi_{ij}^0 + \chi_{ij}^{3\dagger}\chi_{ij}^3\big). \tag{20}$$

Comparing Eqs. (19) and (20) allows us to make the identification

$$\begin{aligned} &i\big(S_i^+S_j^- - S_i^+S_j^-\big) = \chi_{ij}^{0\dagger}\chi_{ij}^3 + \chi_{ij}^{3\dagger}\chi_{ij}^0, \\ &S_i^+S_j^- + S_i^+S_j^- = -\chi_{ij}^{0\dagger}\chi_{ij}^0 + \chi_{ij}^{3\dagger}\chi_{ij}^3. \end{aligned} \tag{21}$$

Table 1
Operator equivalence rules

Spin basis	Valence bond basis
$\mathbf{S}_i \cdot \mathbf{S}_j$	$-\frac{3}{4}\chi^{0\dagger}_{ij}\chi^{0}_{ij} + \frac{1}{4}\boldsymbol{\chi}^{\dagger}_{ij}\cdot\boldsymbol{\chi}_{ij}$
$\mathbf{S}_i \cdot \mathbf{S}_j - \frac{1}{4}$	$-\chi^{0\dagger}_{ij}\chi^{0}_{ij}$
$\mathbf{S}_i - \mathbf{S}_j$	$i(\chi^{0\dagger}_{ij}\boldsymbol{\chi}_{ij} - \boldsymbol{\chi}^{\dagger}_{ij}\chi^{0}_{ij})$
$\mathbf{S}_i + \mathbf{S}_j$	$i\boldsymbol{\chi}^{\dagger}_{ij}\times\boldsymbol{\chi}_{ij}$
$S^+_i S^-_j + S^-_i S^+_j$	$-\chi^{0\dagger}_{ij}\chi^{0}_{ij} + \chi^{3\dagger}_{ij}\chi^{3}_{ij}$
$i(S^+_i S^-_j - S^-_i S^+_j)$	$\chi^{0\dagger}_{ij}\chi^{3}_{ij} + \chi^{3\dagger}_{ij}\chi^{0}_{ij}$

We have so far confined our discussion to a system of two spins. Nonetheless, everything derived up to this point applies equally well to *any* two spins of a many-spin system. In that sense, the results summarized in Table 1 are valid generally: we simply assert that there are operators χ^{μ}_{ij} associated with *every* pair of sites in the lattice. The only remaining step is to determine what the appropriate anticommutator algebra is for operators with one site index in common. A straightforward calculation shows that

$$\big[\chi^{\rho}_{ij}, \chi^{\mu\dagger}_{kj}\chi^{\nu\dagger}_{il}\big]|\text{vac}\rangle = \frac{1}{2}T^{\lambda\mu\rho\nu}\chi^{\lambda\dagger}_{kl}|\text{vac}\rangle, \tag{22}$$

where $T^{\lambda\mu\rho\nu} = \frac{1}{2}\operatorname{tr}\tau^{\lambda\dagger}\tau^{\mu}\tau^{\rho\dagger}\tau^{\nu}$ and summation over the repeated index λ is implied.

3. $S = 0$ valence bond basis

For a system of many SU(2) spins, the structure of the Hilbert space can be determined from the product rule $\frac{1}{2}\otimes S = (S-\frac{1}{2})\oplus(S+\frac{1}{2})$, where S denotes the $(2S+1)$-degenerate spin-S state. Thus,

$$\begin{aligned}
&\frac{1}{2}\otimes\frac{1}{2} = 0\oplus 1,\\
&\frac{1}{2}\otimes\frac{1}{2}\otimes\frac{1}{2} = \frac{1}{2}\oplus\frac{1}{2}\oplus\frac{3}{2},\\
&\frac{1}{2}\otimes\frac{1}{2}\otimes\frac{1}{2}\otimes\frac{1}{2} = 0\oplus 0\oplus 1\oplus 1\oplus 2,\\
&\vdots\\
&\underbrace{\frac{1}{2}\otimes\frac{1}{2}\otimes\frac{1}{2}\otimes\cdots\otimes\frac{1}{2}}_{2N\text{ times}} = \prod_{S=0}^{N}\underbrace{S\oplus\cdots\oplus S}_{C_S^{(N)}\text{ times}}.
\end{aligned} \tag{23}$$

The number, $C_S^{(N)}$, of S-blocks that appears in the Hilbert space of $2N$ spins is given in Table 2. The number of states in the singlet sector, $C_0^{(N)} = \frac{1}{N+1}\binom{2N}{N} = \frac{(2N)!}{N!(N+1)!}$, represents a small fraction of the total number of states, $\sum_{S=0}^{N}(2S+1)C_S^{(N)} = 2^{2N}$.

To construct a valence bond state in the singlet sector (as per Eq. (1)), we simply group the spins into N pairs and, starting from the bosonic vacuum, act with $\chi^{0\dagger}_{ij}$ for each pair (i,j).

Table 2
Values of the coefficient $C_S^{(N)}$, representing the number of spin-S blocks in the Hilbert space of N pairs of SU(2) spins

	0	1/2	1	3/2	2	5/2	3	7/2		
		1								
1	1		1							
		2		1						
2	2		3		1					
		5		4		1				
3	5		9		5		1			
		14		14		6		1		
4	14		28		20		7		1	
		42		48		27		8		1
5	42		90		75		35		9	
		132		165		120		24		10
6	132		297		285		144		34	

The number of such states is

$$T_N = \frac{1}{N!}\binom{2N}{2}\binom{2N-2}{2}\cdots\binom{2}{2} = \frac{(2N)!}{2^N(N!)}. \tag{24}$$

This dwarfs the number of independent states in the singlet sector for large N ($T_N \gg C_0^{(N)}$).

As a consequence of the overcompleteness, linear combinations of valence bond states are generally not unique—an ambiguity related to the fact that linear independence fails even at the level of two singlets:

$$\chi_{il}^{0\dagger}\chi_{jk}^{0\dagger} + \chi_{ij}^{0\dagger}\chi_{kl}^{0\dagger} + \chi_{lj}^{0\dagger}\chi_{ik}^{0\dagger} = 0. \tag{25}$$

In the case of two spins ($N = 1$), there is a single tiling ($T_1 = 1$) corresponding to the unique singlet state ($C_0^{(1)} = 1$). In the case of four spins ($N = 2$), the number of tilings ($T_2 = 3$) exceeds the number of physical singlet states ($C_0^{(2)} = 2$) by one. It is useful to eliminate this superfluous state. For concreteness, let us suppose that the lattice of $2N$ spins is described as the union $A \cup B$ of sites $A = \{i_1, i_2, \ldots, i_N\}$ and $B = \{j_1, j_2, \ldots, j_N\}$. This is simply a labeling trick and does not depend on the lattice being bipartite. We restrict the basis to include only those valence bonds that connect A sites to B sites. This is possible since any unwanted AA and BB bonds can be replaced by two AB bonds via Eq. (25).

The AB valence bond basis is intimately related to $\mathcal{S}_N$, the symmetric group of degree N. There is a one-to-one correspondence between the bond tilings and the permutations that are the elements of $\mathcal{S}_N$. This correspondence holds because every bond tiling can be thought of as a rearrangement of the B labels. That is, for each $P \in \mathcal{S}_N$, there is a state

$$|P\rangle = \hat{P}^\dagger|\text{vac}\rangle = \prod_{n=1}^{N} \chi_{i_n, j_{P_n}}^{0\dagger}|\text{vac}\rangle. \tag{26}$$

It follows that there are $\tilde{T}_N = N!$ such states. For example, Fig. 2 shows the $3! = 6$ AB bond configurations for $N = 3$. These states are indexed by the permutations

$$P = (1)(2)(3), \qquad P = (1)(2\ 3), \qquad P = (1\ 2)(3),$$
$$P = (1\ 2\ 3), \qquad P = (3\ 2\ 1), \qquad P = (1\ 3)(2),$$

written here in cycle notation.

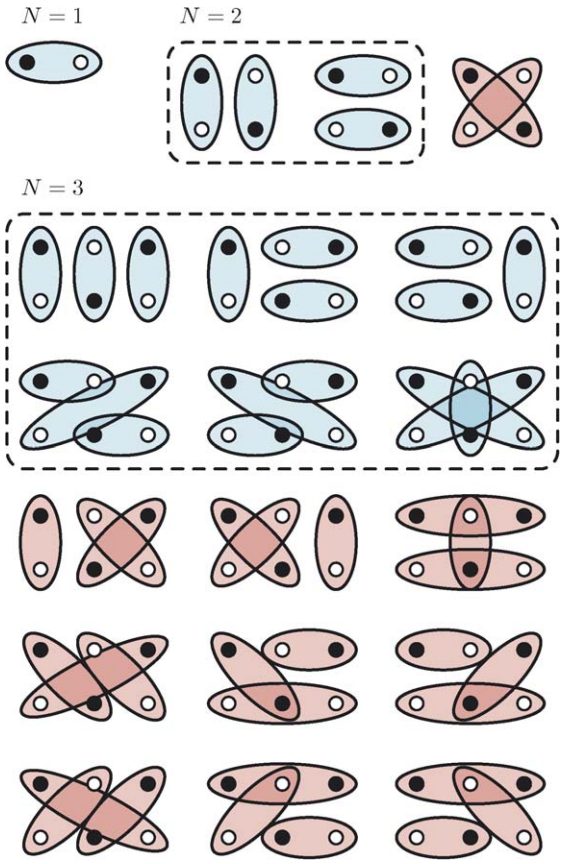

Fig. 2. The set of all possible bond tilings, $T_N = (2N)!/2^N N!$ in number, is shown for $N = 1, 2, 3$. The restricted set of AB tilings (blue) numbers $\tilde{T}_N = N!$, which still exceeds the number of true singlet states. A and B sites are shown as filled and open circles, respectively.

The restriction to the AB basis is useful in that it gives us a systematic way to fix the phase of each state. This is an issue because the singlet is a directed bond: $\chi^0_{ji} = -\chi^0_{ij}$ and $\boldsymbol{\chi}_{ji} = \boldsymbol{\chi}_{ij}$. We adopt the convention that the canonical form of the operator χ^μ_{ij} has $i \in A$ and $j \in B$, as in Eq. (26). As we shall see in Section 5, all overlaps of AB valence bond states are positive definite, which is not true in the unrestricted basis [39].

One disadvantage to the AB basis is that the identity operator in the $S = 0$ subspace has a complicated form. In the unrestricted basis, it is diagonal,

$$\hat{1}_0 = \frac{2^N}{(N+1)!} \sum_v |v\rangle\langle v|, \tag{27}$$

with a normalization $T_N / C_0^{(N)}$, but the process of eliminating all AA and BB bonds from Eq. (27) introduces offdiagonal terms. For $N = 2$ and $N = 3$, the identity operators are

$$\hat{1}_0 = \frac{2}{3} \sum_{P,Q} |P\rangle \begin{pmatrix} 2 & -1 \\ -1 & 2 \end{pmatrix}_{P,Q} \langle Q| \tag{28}$$

and

$$\hat{1}_0 = \frac{1}{3}\sum_{P,Q}|P\rangle \begin{pmatrix} 4 & -1 & -1 & 0 & 0 & -1 \\ -1 & 4 & 0 & -1 & -1 & 0 \\ -1 & 0 & 4 & -1 & -1 & 0 \\ 0 & -1 & -1 & 4 & 0 & -1 \\ 0 & -1 & -1 & 0 & 4 & -1 \\ -1 & 0 & 0 & -1 & -1 & 4 \end{pmatrix}_{P,Q} \langle Q|. \tag{29}$$

In these examples, the rows and columns of the coefficient matrices are arranged to match the ordering of the permutations in Fig. 2. The entries are $(2N)!/2^{N-1}(N!)^2 - 1$ along the main diagonal and 0 or -1 elsewhere, which is a consequence of there being at most one AA/BB set to unravel. For $N > 3$, the situation is more complicated, and we do not know of a simple general expression for $\hat{1}_0$. In most practical applications, however, such an expression is not needed.

It is possible to construct basis sets that are still more restrictive (i.e., having fewer states than the AB basis). There is a hierarchy of linear dependence relations (similar to Eq. (25)) for groups of three, four, and higher numbers of singlet bonds, which can be used to further eliminate unwanted states. When carried out to its fullest extent, this elimination procedure leaves a set of valence bond configurations equal in number to the actual number of $S = 0$ states. Explicit construction of the basis in this limit can be accomplished by arranging the lattice sites $i_1, j_1, i_2, j_2, \ldots, i_N, j_N$ on a ring and keeping only the AB tilings that produce no bond crossings. Note that even this minimal set contains long bonds connecting sites that are macroscopically separated, which suggests that bonds on all length scales are required for completeness.

4. Evolution of valence bond states

Now suppose that we have a Hamiltonian of the form

$$\hat{H} = \sum_{ij} J_{ij}\hat{H}_{ij} - \sum_{ijkl} K_{ijkl}\hat{H}_{ij}\hat{H}_{kl} + \cdots \tag{30}$$

with second-, forth-, and potentially higher-order spin interactions [40]. Here, $\hat{H}_{ij}$ is defined as in Eq. (12). In order to understand how an arbitrary state evolves under $\hat{H}$, we need to know how a given valence bond state evolves under repeated applications of $-\hat{H}_{ij}$.

Depending on the circumstances, $-\hat{H}_{ij}$ is either a diagonal operation that leaves the overall configuration unchanged or an off-diagonal operation that maps two bonds to their complementary tiling:

$$\left(\frac{1}{4} - \mathbf{S}_i \cdot \mathbf{S}_j\right)[i,j] = [i,j], \tag{31}$$

$$\left(\frac{1}{4} - \mathbf{S}_i \cdot \mathbf{S}_j\right)[l,i][j,k] = [i,j][k,l]. \tag{32}$$

This result, which is true in the unrestricted basis, has long been known [3]. It will be instructive to see how it emerges within our formalism and how it is modified to accommodate the restriction to AB bonds.

Let us start with the state $|P\rangle = \hat{P}^\dagger|\text{vac}\rangle$, where $\hat{P}^\dagger$ is the operator string defined in Eq. (26). Then,

$$-\hat{H}_{ij}|P\rangle = \chi^{0\dagger}_{ij}\chi^0_{ij}\hat{P}^\dagger|\text{vac}\rangle = \chi^{0\dagger}_{ij}\big[\chi^0_{ij}, \hat{P}^\dagger\big]|\text{vac}\rangle. \tag{33}$$

There are two possibilities to consider in evaluating the anticommutator: (i) if there is already a bond connecting the active sites (i.e., $\hat{P}^\dagger = \cdots \chi^{0\dagger}_{ij} \cdots$), then only two operators play a role in the anticommutator. In this case, Eq. (10) is the appropriate rule to apply, and Eq. (33) simplifies to

$$\chi^{0\dagger}_{ij}\chi^{0}_{ij}|P\rangle = |P\rangle. \tag{34}$$

(ii) If the active sites are each connected elsewhere (i.e., $\hat{P}^\dagger = \cdots \chi^{0\dagger}_{il} \cdots \chi^{0\dagger}_{kj} \cdots$ for some $k \in A$, $l \in B$), then three operators are involved. This necessitates the use of Eq. (22) and leads to

$$\chi^{0\dagger}_{ij}\chi^{0}_{ij}|P\rangle = \frac{1}{2}\chi^{0\dagger}_{i_1 j_{P1}} \cdots \chi^{0\dagger}_{ij} \cdots \chi^{0\dagger}_{kl} \cdots \chi^{0\dagger}_{i_N j_{PN}}|\text{vac}\rangle. \tag{35}$$

The new state on the right-hand side is itself a valence bond state (different from $|P\rangle$), since it consists of N operators and none of its $2N$ indices are repeated. If $i \in A$ and $j \in B$, then this state contains only AB bonds.

A reconfiguration of the bonds manifests itself as a change in the permutation indexing the state. If $i = i_n$ and $j = j_m$ are in opposite sublattices, then Eqs. (34) and (35) are summarized by the compact update rule

$$-\hat{H}_{i_n j_m}|P\rangle = \left(\frac{1}{2}\right)^{1-\delta_{Pn,m}} \big|(Pn\ m)P\big\rangle, \tag{36}$$

where the term $(Pn\ m)$ inside the ket is a 2-cycle acting on P (the effect of which is to swap the labels j_{Pn} and j_m). Eq. (36) makes clear that the Hamiltonian is an identity operation whenever it acts on a preexisting bond; otherwise it induces a single transposition and a multiplicative factor $\frac{1}{2}$. Note that the transposition itself depends on P.

If, however, i and j are in the same sublattice, then the $\chi^{0\dagger}_{ij}\chi^{0\dagger}_{kl}$ operators in Eq. (35) have to be eliminated in favour of AB bonds. This leads to

$$-\hat{H}_{i_n i_m}|P\rangle = \frac{1}{2}|P\rangle - \left(\frac{1}{2}\right)^{1-\delta_{n,m}} \big|(Pn\ Pm)P\big\rangle \tag{37}$$

and

$$-\hat{H}_{j_n j_m}|P\rangle = \frac{1}{2}|P\rangle - \left(\frac{1}{2}\right)^{1-\delta_{n,m}} \big|(n\ m)P\big\rangle. \tag{38}$$

These "frustrating" interactions create a linear superposition of states, rather than just a rearrangement of bonds. They also introduce bond configurations with negative weight, violating the conditions of the Marshall sign theorem [41]. Fig. 3 illustrates the frustrating and nonfrustrating bond flips that can occur.

If there are no frustrating interactions in the Hamiltonian then the ground state can be written as a superposition of valence bond states $|\psi\rangle = \sum_P c_P|P\rangle$ with all $c_P \geqslant 0$. In that special case, Monte Carlo simulation is sign-problem-free.

5. Overlaps and matrix elements of valence bond states

It follows from Eq. (26) that the overlap of any two valence bond states is equal to the vacuum-state expectation value of a length-$2N$ operator string:

$$\langle Q|P\rangle = \langle\text{vac}|\chi^{0}_{i_N,j_{QN}} \cdots \chi^{0}_{i_2,j_{Q2}}\chi^{0}_{i_1,j_{Q1}}\chi^{0\dagger}_{i_1,j_{P1}}\chi^{0\dagger}_{i_2,j_{P2}} \cdots \chi^{0\dagger}_{i_N,j_{PN}}|\text{vac}\rangle. \tag{39}$$

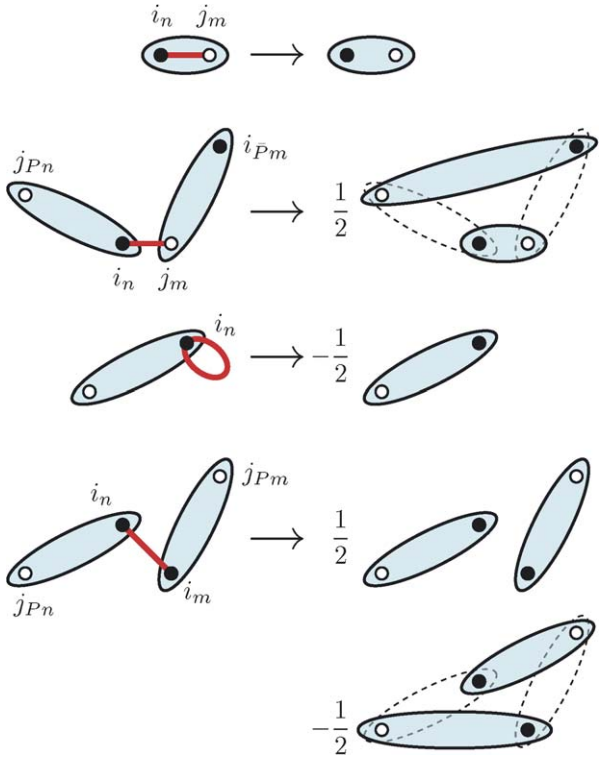

Fig. 3. AB valence bonds obey a simple set of update rules when acted on with an isotropic spin interaction term. Here the update rules for $1/4 - \mathbf{S}_i \cdot \mathbf{S}_j$ are summarized. The red bar denotes the interaction between the spins at sites i and j. The site labels follow the notation in Eqs. (36) and (37). Of the terms that involve a reconfiguration of the bonds (dashed outlines indicate the previous bond locations), one corresponds to an exchange of j_{Pn} and j_m and the other j_{Pn} and j_{Pm}.

The creation and annihilation operators can be shuffled past one another so long as they share no indices in common. The maximal such rearrangement leaves the string grouped into several linked chains of operators; these are related to the disjoint cycles of the composite permutation $\bar{Q}P$ (we use the notation $\bar{Q} = Q^{-1}$ to denote the inverse permutation of Q) and define a set of directed loops (with $\bar{Q}P$ defining the proper order), e.g.,

$$i_1 \to j_{P1} \to i_{\bar{Q}P1} \to j_{P\bar{Q}P1} \to i_{\bar{Q}P\bar{Q}P1} \to \cdots \to i_{(\bar{Q}P)^k 1} = i_1. \tag{40}$$

Fig. 4 illustrates the construction. Each of these loops is even in length—constituting a chain with equal numbers of links from P and Q. The cycle decomposition is related to the loop membership of the site indices by

$$\begin{aligned}
&n \overset{\bar{Q}P}{\sim} \bar{P}m \;\Leftrightarrow\; i_n \text{ and } j_m \text{ in same loop},\\
&n \overset{\bar{Q}P}{\sim} m \;\Leftrightarrow\; i_n \text{ and } i_m \text{ in same loop},\\
&\bar{P}n \overset{\bar{Q}P}{\sim} \bar{P}m \;\Leftrightarrow\; j_n \text{ and } j_m \text{ in same loop}.
\end{aligned} \tag{41}$$

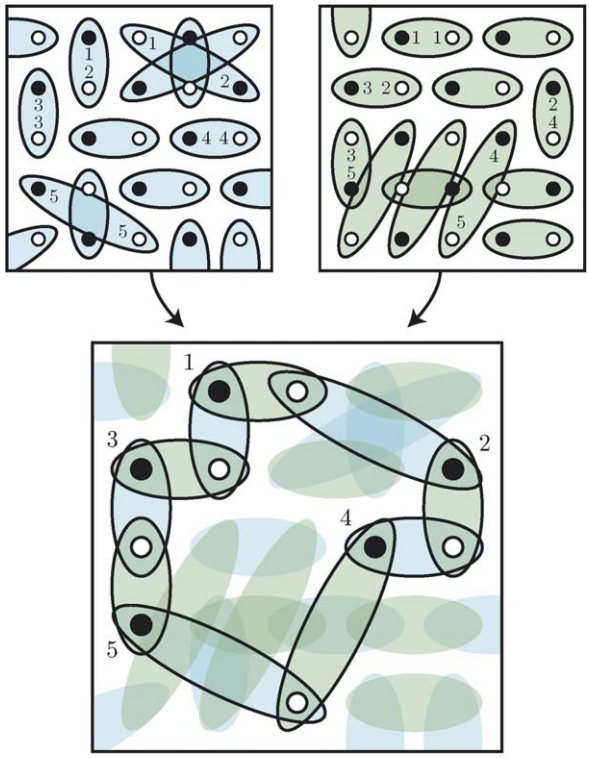

Fig. 4. The top-left and top-right panels illustrate valence bond states $|P\rangle$ and $|Q\rangle$ corresponding to the permutations $P = (1\ 2)(3)(4)(5)\cdots$ and $Q = (1)(2\ 4\ 5\ 3)\cdots$; the sites $i_1, i_2, \ldots, i_5$ (filled circles) and $j_1, j_2, \ldots, j_5$ (open circles) are numbered accordingly (in no particular order). The overlap $\langle Q|P\rangle$ between these states is literally that: a superposition of the two bond configurations. Since the end point of one bond is always the starting point of another, a set of closed bond paths is formed. These are in one-to-one correspondence with the disjoint cycles of $\bar{Q}P$. In this example, $\bar{Q}P = (1\ 2\ 4\ 5\ 3)\cdots$ has a cycle of length 5 and a corresponding bond loop of length 10.

We use the notation $x \overset{\bar{Q}P}{\sim} y$ to indicate that x and y are in the same cycle of $\bar{Q}P$. All the loops taken together form a set of closed paths covering the lattice. Hence,

$$\sum_{k=1}^{N} 2k \cdot n_k = 2N, \tag{42}$$

where n_k is the number of loops of length $2k$ (or the number of k-cycles in $\bar{Q}P$).

The value of the overlap can be computed by way of a simple decimation scheme [36,37]. Each loop can be eliminated by repeated application of Eqs. (10) and (22), specialized to the case of $\rho = \nu = \mu = 0$:

$$\left[\chi^{0}_{ij}, \chi^{0\dagger}_{ij}\right]|\mathrm{vac}\rangle = |\mathrm{vac}\rangle \tag{43}$$

and

$$\left[\chi^{0}_{ij}, \chi^{0\dagger}_{kj}\chi^{0\dagger}_{il}\right]|\mathrm{vac}\rangle = \frac{1}{2}\chi^{0\dagger}_{kl}|\mathrm{vac}\rangle. \tag{44}$$

For a loop of length $2k$, $k-1$ applications of Eq. (44) removes $2k-2$ links and yields $k-1$ factors of $1/2$. The final two operators are removed with a single application of Eq. (43), leaving $\langle \mathrm{vac}|\mathrm{vac}\rangle = 1$. Hence,

$$\langle Q|P\rangle = \prod_{l=1}^{N}\left(\frac{1}{2^{k-1}}\right)^{n_k} = \frac{2^{\sum_{l=1}^{N} n_k}}{2^{\sum_{l=1}^{N} k\cdot n_k}} = 2^{N_{\circlearrowleft}-N}, \tag{45}$$

where we have used Eq. (42) and defined the total number of loops $N_{\circlearrowleft} = \sum_{k=1}^{N} n_k$.

Similar arguments can be used to compute the matrix elements of a spin-rotation-invariant operator $\hat{O}$. In general, such an operator acting on a valence bond state produces a linear superposition of states with modified bond configurations:

$$\hat{O}|P\rangle = \sum_{P'} O_{P,P'}|P'\rangle. \tag{46}$$

(The situation is more complicated if $\hat{O}$ generates states outside the $S=0$ sector; this is discussed further in Section 8.) Since the basis is overcomplete, the coefficients $O_{P,P'}$ are not unique and $O_{P,P'} \neq \langle P|\hat{O}|P'\rangle$, as would be the case in an orthonormal basis. Eqs. (45) and (46) imply that matrix elements are related to changes in the loop number:

$$\frac{\langle Q|\hat{O}|P\rangle}{\langle Q|P\rangle} = \sum_{P'} O_{P,P'} 2^{N'_{\circlearrowleft}-N_{\circlearrowleft}}. \tag{47}$$

Here, $N_{\circlearrowleft}$ is the number of cycles in $\bar{Q}P$ and $N'_{\circlearrowleft}$ the number in $\bar{Q}P'$.

Evaluation of Eq. (47) requires some general rules for how the number of cycles changes as $P \to P'$. Since the permutation $P'\bar{P}$ can always be decomposed into a product of transpositions, it suffices to consider the situation where the two states differ by a single transposition. In that case, $N'_{\circlearrowleft} - N_{\circlearrowleft} = \pm 1$ (see Appendix A), since a transposition $(n\ m)$ either merges the two cycles that each contain one of $\bar{P}n$ and $\bar{P}m$ or splits the single cycle that contains them both. This can be expressed formally as

$$\frac{\langle Q|(n\ m)P\rangle}{\langle Q|P\rangle}\left(\frac{1}{2}\right)^{1-\delta_{n,m}} = \begin{cases} 1 & \text{if } \bar{P}n \overset{\bar{Q}P}{\sim} \bar{P}m, \\ \frac{1}{4} & \text{otherwise.} \end{cases} \tag{48}$$

Here, the delta function takes care of the possibility that $n=m$, which corresponds to no transposition at all.

Applying this result to Eqs. (36)–(38) (with the right-hand side of Eq. (48) interpreted according to (41)) gives

$$\frac{\langle Q|\chi_{ij}^{0\dagger}\chi_{ij}^{0}|P\rangle}{\langle Q|P\rangle} = \frac{1}{4}\left(1 - 3\epsilon_{ij}\delta^{\alpha_i\alpha_j}\right), \tag{49}$$

where α_i and α_j are unique labels for the loops passing through sites i and j. We have introduced the notation

$$\epsilon_{ij} = \begin{cases} -1 & \text{if } i,\ j \text{ are in different sublattices,} \\ +1 & \text{otherwise.} \end{cases} \tag{50}$$

To clarify, let us rederive Eq. (49) by considering explicitly the effect of $\chi_{ij}^{0\dagger}\chi_{ij}^{0}$ acting to the right on $|P\rangle$ and how the overlap of the resulting state with $\langle Q|$ differs from the loop structure

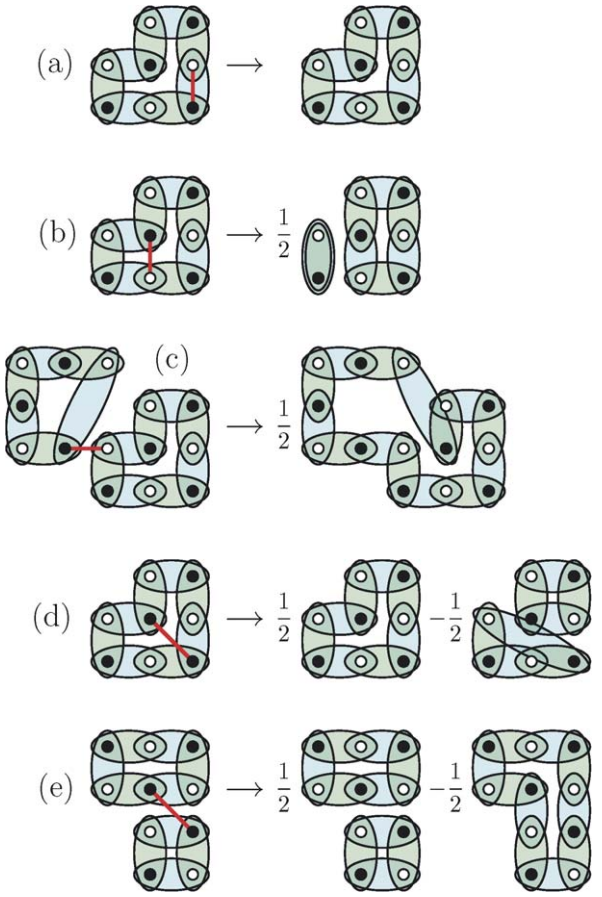

Fig. 5. The operator $\chi^{0\dagger}_{ij}\chi^{0}_{ij} = 1/4 - \mathbf{S}_i \cdot \mathbf{S}_j$ causes a rearrangement of bonds, as shown in Fig. 3. Thus, its matrix element can be understood in terms of joining or splitting loops.

of $\langle Q|P\rangle$. We distinguish between the AB case, in which the sites i and j are in different sublattices, and the AA/BB case, in which they are in the same sublattice. For AB operators, the possibilities are illustrated in Fig. 5(a)–(c). If the two sites belong to the same loop then either an offdiagonal operation splits the loop, giving a contribution $(1/2)(2^1) = 1$ (following Eq. (47)) or a diagonal operation leaves the loop unchanged, also giving $(1)(2^0) = 1$. If the two sites belong to different loops then the offdiagonal operation joins the two loops, giving $(1/2)(2^{-1}) = 1/4$. Combining these results gives

$$\frac{\langle Q|\chi^{0\dagger}_{ij}\chi^{0}_{ij}|P\rangle}{\langle Q|P\rangle} = \delta^{\alpha_i\alpha_j} + \frac{1}{4}\left(1 - \delta^{\alpha_i\alpha_j}\right) = \frac{3}{4}\delta^{\alpha_i\alpha_j} + \frac{1}{4}. \tag{51}$$

For AA/BB operators, the possible bond reconfigurations are illustrated in Fig. 5(d) and (e). The two sites are either in the same loop, giving $(1/2)(2^0 - 2^1) = -1/2$, or in different loops, giving $(1/2)(2^0 - 2^{-1}) = 1/4$. The result,

$$\frac{\langle Q|\chi^{0\dagger}_{ij}\chi^{0}_{ij}|P\rangle}{\langle Q|P\rangle} = -\frac{1}{2}\delta^{\alpha_i\alpha_j} + \frac{1}{4}\left(1 - \delta^{\alpha_i\alpha_j}\right) = -\frac{3}{4}\delta^{\alpha_i\alpha_j} + \frac{1}{4}, \tag{52}$$

differs from Eq. (51) by only a sign. Using ϵ_{ij} to account for the difference in sign yields Eq. (49).

The same formal manipulations that lead from Eq. (48) to Eq. (49) can be chained together to evaluate a long operator sequence one transposition at a time. For example, taking $i = i_n \in A$ and $j = j_m \in B$, we get

$$\frac{\langle Q|\hat{O}\chi_{ij}^{0\dagger}\chi_{ij}^{0}|P\rangle}{\langle Q|P\rangle} = \frac{\langle Q|\hat{O}|(Pn\,m)P\rangle}{\langle Q|P\rangle}\left(\frac{1}{2}\right)^{1-\delta_{Pn,m}} = \frac{\langle Q|\hat{O}|P'\rangle}{\langle Q|P'\rangle}\frac{\langle Q|P'\rangle}{\langle Q|P\rangle}\left(\frac{1}{2}\right)^{1-\delta_{Pn,m}}$$
$$= \frac{\langle Q|\hat{O}|P'\rangle}{\langle Q|P'\rangle}\frac{1}{4}\left(1+3\delta^{\alpha_i\alpha_j}\right), \tag{53}$$

where $P' = (Pn\,m)P$ describes the new bond configuration after one transposition. For arbitrary site indices, the expression reads

$$\frac{\langle Q|\hat{O}\chi_{ij}^{0\dagger}\chi_{ij}^{0}|P\rangle}{\langle Q|P\rangle} = \frac{1}{4}(1+\epsilon_{ij})\frac{\langle Q|\hat{O}|P\rangle}{\langle Q|P\rangle} - \epsilon_{ij}\frac{\langle Q|\hat{O}|P'\rangle}{\langle Q|P'\rangle}\frac{1}{4}\left(1+3\delta^{\alpha_i\alpha_j}\right). \tag{54}$$

6. Spin correlation functions

So long as the ground state of the spin system is a global singlet, its wavefunction can be written as a linear superposition of valence bond states: $|\psi\rangle = \sum_P c_P|P\rangle$. Accordingly, operator expectation values have the form

$$\langle\hat{O}\rangle = \frac{\langle\psi|\hat{O}|\psi\rangle}{\langle\psi|\psi\rangle} = \frac{\sum_{P,Q} W(P,Q)\frac{\langle Q|\hat{O}|P\rangle}{\langle Q|P\rangle}}{\sum_{P,Q} W(P,Q)}, \tag{55}$$

with $P, Q \in \mathcal{S}_N$ and $\hat{O}$ some operator of interest. The quantity $W(P,Q) = c_Q c_P\langle Q|P\rangle$ may be determined variationally [13] or it may arise as a sampling weight in the context of a Monte Carlo projection scheme [33]. The matrix element $\langle Q|\hat{O}|P\rangle/\langle Q|P\rangle$ is related to the properties of the loops that are formed when the singlet tilings of the two states are superimposed. In fact, since its value depends only on the properties of the loops, the individual valence bond states can be abstracted away entirely, leaving what is essentially a loop estimator for $\hat{O}$; we denote this function $O_{\mathcal{L}}$. In this way of thinking, Eq. (55) can best be understood as $\langle\hat{O}\rangle = \langle O_{\mathcal{L}}\rangle_W$, an ensemble average of $O_{\mathcal{L}}$ in the gas of fluctuating loops [42,43].

In this section, we want to determine the loop estimators for the spin operators $\mathbf{S}_i\cdot\mathbf{S}_j$ and $(\mathbf{S}_i\cdot\mathbf{S}_j)(\mathbf{S}_k\cdot\mathbf{S}_l)$. All the work to compute the second order result has already been done. Since $\mathbf{S}_i\cdot\mathbf{S}_j = \frac{1}{4} - \chi_{ij}^{0\dagger}\chi_{ij}^{0}$, comparison with Eq. (49) immediately yields

$$(\mathbf{S}_i\cdot\mathbf{S}_j)_{\mathcal{L}} = \frac{3}{4}\epsilon_{ij}\delta^{\alpha_i\alpha_j}. \tag{56}$$

For the fourth order result, we begin by specializing Eq. (54) to the case $\hat{O} = \chi_{kl}^{0\dagger}\chi_{kl}^{0}$, which gives

$$\frac{\langle Q|\chi_{ij}^{0\dagger}\chi_{ij}^{0}\chi_{kl}^{0\dagger}\chi_{kl}^{0}|P\rangle}{\langle Q|P\rangle} = \frac{1}{16}\left(1-\epsilon_{ij}3\delta^{\alpha_i'\alpha_j'}\right)\left(1-\epsilon_{kl}3\delta^{\alpha_k\alpha_l}\right)$$
$$+\frac{3}{16}(1+\epsilon_{ij})\epsilon_{kl}\left(\delta^{\alpha_i'\alpha_j'}-\delta^{\alpha_i\alpha_j}\right). \tag{57}$$

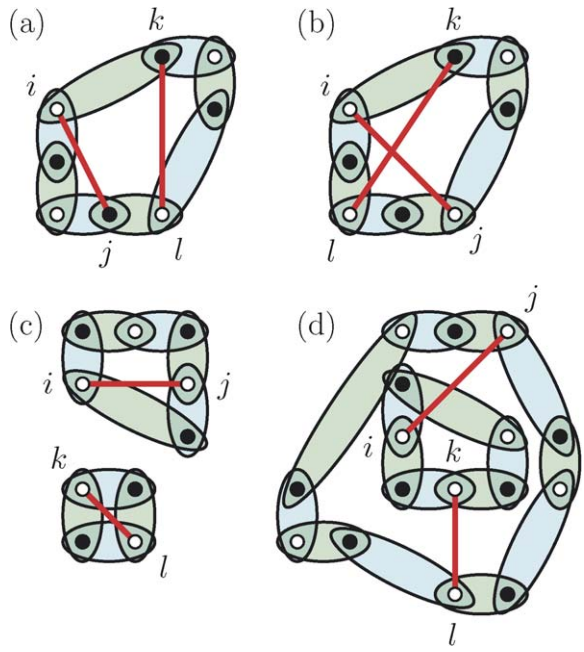

Fig. 6. The expectation value of $\epsilon_{ij}\epsilon_{kl}(\mathbf{S}_i \cdot \mathbf{S}_j)(\mathbf{S}_k \cdot \mathbf{S}_l)$ is nonzero only if (i, j) and (k, l) connect one or two loops. For one loop, the value is either $9/16$ or $-3/16$ depending on whether k and l are in the (a) same or (b) different loop segments connecting i and j. For two loops, the value is either $9/16$ or $3/16$ depending on whether the interactions leave the loops (c) disjoint or (d) connected.

Here, α labels the loops in $\bar{Q}P$ and α' labels the loops in $\bar{Q}P'$ where P' is the modified configuration after $\chi^{0\dagger}_{kl}\chi^{0}_{kl}$ has acted on $|P\rangle$. Making use of

$$\chi^{0\dagger}_{ij}\chi^{0}_{ij}\chi^{0\dagger}_{kl}\chi^{0}_{kl} = \frac{1}{16} - \frac{1}{4}\mathbf{S}_i \cdot \mathbf{S}_j - \frac{1}{4}\mathbf{S}_k \cdot \mathbf{S}_l + (\mathbf{S}_i \cdot \mathbf{S}_j)(\mathbf{S}_k \cdot \mathbf{S}_l) \tag{58}$$

and Eq. (56), we arrive at

$$\big[(\mathbf{S}_i \cdot \mathbf{S}_j)(\mathbf{S}_k \cdot \mathbf{S}_l)\big]_{\mathcal{L}} = \epsilon_{ij}\epsilon_{kl}\left[\frac{3}{16}\big(\delta^{\alpha'_i\alpha'_j} - \delta^{\alpha_i\alpha_j}\big) + \frac{9}{16}\delta^{\alpha'_i\alpha'_j}\delta^{\alpha_k\alpha_l}\right]. \tag{59}$$

There is no contribution when $\delta^{\alpha'_i\alpha'_j} = \delta^{\alpha_i\alpha_j} = 0$. Hence, the estimator is nonzero only if all four site indices belong to the same loop or if there are two indices in each of two loops. The possible configurations are shown in Fig. 6. Note that if the vertices (i, j) and (k, l) reside in different loops or if they are in the same loop but remain unlinked (i.e., there is a path along the loop from i to j that does not encounter k or l) then $\delta^{\alpha'_i\alpha'_j} = \delta^{\alpha_i\alpha_j}$. This equality holds because the operation on (k, l) does not disrupt the loop structure at sites i and j. In this case, the bracketed term on the right-hand side is $\frac{9}{16}\delta^{\alpha_i\alpha_j}$. Otherwise, $\delta^{\alpha'_i\alpha'_j} = 1 - \delta^{\alpha_i\alpha_j}$ and the bracketed term is $\frac{3}{16}(1 - 2\delta^{\alpha_i\alpha_j})$.

The undesirable aspect of Eq. (59) is that it is history-dependent. There are several cases to consider because α' references the loop configuration as it exists after application of the (k, l) vertex. Ideally, we want to reexpress the estimator in a way that eliminates the α' labels. This can

be accomplished—at the expense of introducing a new quantity A—as follows:

$$\big[(\mathbf{S}_i\cdot\mathbf{S}_j)(\mathbf{S}_k\cdot\mathbf{S}_l)\big]_{\mathcal{L}} = \epsilon_{ij}\epsilon_{kl}\bigg[-\frac{3}{8}(1+2A)\delta^{\alpha_i\alpha_j}\delta^{\alpha_j\alpha_k}\delta^{\alpha_k\alpha_l} + \frac{9}{16}\delta^{\alpha_i\alpha_j}\delta^{\alpha_k\alpha_l} + \frac{3}{16}\big(\delta^{\alpha_i\alpha_k}\delta^{\alpha_j\alpha_l}+\delta^{\alpha_i\alpha_l}\delta^{\alpha_j\alpha_k}\big)\bigg]. \tag{60}$$

$A = 0, 1$ is a topological term whose value is nonzero when traversal of the loop reveals an antisymmetric permutation of the site labels i, j, k, l. It distinguishes the Fig. 6(b) configuration ($A = 1$) from that of Fig. 6(a) ($A = 0$). For spin correlations of order four and above, the loop estimator is no longer simply a function of the loop labels α_i.

We can make use of Eqs. (56) and (60) to calculate powers of $\hat{\mathbf{M}} = \sum_{i\in A}\mathbf{S}_i - \sum_{j\in B}\mathbf{S}_j$, which on a bipartite lattice corresponds to the staggered magnetization. At second order, we have $\hat{\mathbf{M}}^2 = \sum_{ij}\epsilon_{ij}\mathbf{S}_i\cdot\mathbf{S}_j$ and hence, via Eq. (56),

$$\mathbf{M}^2_{\mathcal{L}} = \frac{\langle Q|\hat{\mathbf{M}}^2|P\rangle}{\langle Q|P\rangle} = \frac{3}{4}\sum_{\alpha=1}^{N_{\circlearrowleft}} L_\alpha^2. \tag{61}$$

This follows because there are L_α^2 ways to choose two sites from a loop of length L_α. In the same way, $\hat{\mathbf{M}}^4 = \sum_{ijkl}\epsilon_{ij}\epsilon_{kl}(\mathbf{S}_i\cdot\mathbf{S}_j)(\mathbf{S}_k\cdot\mathbf{S}_l)$ can be computed using Eq. (60). The only complication is the case where i, j, k, l are all in the same loop α. Of the L_α^4 such configurations,

$$L_\alpha\sum_{j=1}^{L_\alpha}\big[2j(L_\alpha - j) - 1\big] = \frac{1}{3}L_\alpha^4 - \frac{4}{3}L_\alpha^2 \tag{62}$$

have weight $-3/16$. The counting reflects the fact that there are L_α ways to fix i and, as j ranges over the loop, $2j(L_\alpha - j) - 1$ ways to place k and l in opposite loop segments. (This includes mixed cases of the form $i = k$, $j \neq l$ which are $A = 1$ in nature, but omits those of the form $i = k$, $j = l$, which are $A = 0$.) The remainder have weight $9/16$. Thus, the total contribution is

$$\sum_\alpha\bigg[\frac{9}{16}\bigg(\frac{2}{3}L_\alpha^4 + \frac{4}{3}L_\alpha^2\bigg) - \frac{3}{16}\bigg(\frac{1}{3}L_\alpha^4 - \frac{4}{3}L_\alpha^2\bigg)\bigg] + \bigg(2\times\frac{3}{16} + \frac{9}{16}\bigg)\sum_{\alpha\neq\beta}L_\alpha^2 L_\beta^2, \tag{63}$$

which simplifies to

$$\mathbf{M}^4_{\mathcal{L}} = \sum_\alpha\bigg(-\frac{5}{8}L_\alpha^4 + L_\alpha^2\bigg) + \frac{15}{16}\bigg(\sum_\alpha L_\alpha^2\bigg)^2. \tag{64}$$

7. Cumulant generating function

Calculating spin correlation functions as we did in the previous section involves keeping track of all possible ways that a given number of site index pairs, $(i, j), (k, l), \ldots$, can be assigned to a set of valence bond loops. For each such assignment, we then have to determine the contribution to the correlation function based on how the loops are reconfigured by the valence bond operators $\chi_{ij}^{0\dagger}\chi_{ij}^0$, $\chi_{kl}^{0\dagger}\chi_{kl}^0, \ldots$. This brute force approach becomes increasingly cumbersome (and errorprone) as the order of the correlation function becomes large. At second and fourth order, the problem is manageable. For $\mathbf{S}_i\cdot\mathbf{S}_j$, there are two distinct configurations—one that contributes

(when i and j are in the same loop) and one that does not (when i and j are in different loops)—and for $(\mathbf{S}_i \cdot \mathbf{S}_j)(\mathbf{S}_j \cdot \mathbf{S}_l)$, there are eight configurations—four that contribute (those shown in Fig. 6) and four that do not. But at sixth order, there are already 33 configurations to consider—an intractable nightmare.

In this section, we present a vastly more simple approach that emerges from a deeper understanding of the relationship between correlation functions and loops. To start, we introduce a new operator

$$\hat{\gamma}_{ij} = \frac{1}{4} + \epsilon_{ij}\mathbf{S}_i \cdot \mathbf{S}_j = \frac{1}{4}(1+\epsilon_{ij}) - \epsilon_{ij}\chi_{ij}^{0\dagger}\chi_{ij}^{0}, \tag{65}$$

which is designed to have a positive definite matrix element, irrespective of the sublattice membership of i and j. What motivates this definition is a desire to compensate for the asymmetry between Eq. (36) and Eqs. (37) and (38), which describe the effect of $\chi_{ij}^{0\dagger}\chi_{ij}^{0}$ on a valence bond state. In the AB case ($\epsilon_{ij} = -1$), the operator $\hat{\gamma}_{ij} = \chi_{ij}^{0\dagger}\chi_{ij}^{0}$ produces only a rearrangement of bonds and leaves the phase of the state unchanged, which is the desired state of affairs; in the AA/BB case ($\epsilon_{ij} = 1$), the operator $\hat{\gamma}_{ij} = \frac{1}{2} - \chi_{ij}^{0\dagger}\chi_{ij}^{0}$ is engineered to behave in exactly the same way, by canceling the first term and changing the sign of the second term on the right-hand side of Eqs. (37) and (38). Pictorially, this amounts to removing the identity part and changing the sign of the transposition part from $-\frac{1}{2}$ to $\frac{1}{2}$ on the right-hand side of the third (bottom) update rule in Fig. 3. The rearrangement of individual singlets is governed by

$$\hat{\gamma}_{ij}[i,j] = \hat{\gamma}_{ii}[i,j] = [i,j], \tag{66}$$

$$\hat{\gamma}_{ij}[i,l][k,j] = \hat{\gamma}_{ik}[i,l][k,j] = \frac{1}{2}[i,j][k,l] \tag{67}$$

for sites $i,k \in A$ and $j,l \in B$. Hence,

$$\hat{\gamma}_{i_n j_m}|P\rangle = 2^{\delta_{Pn,m}-1}\big|(Pn\ m)P\big\rangle, \tag{68}$$

$$\hat{\gamma}_{i_n i_m}|P\rangle = 2^{\delta_{n,m}-1}\big|(Pn\ Pm)P\big\rangle, \tag{69}$$

$$\hat{\gamma}_{j_n j_m}|P\rangle = 2^{\delta_{n,m}-1}\big|(n\ m)P\big\rangle. \tag{70}$$

Since $\hat{\gamma}_{ij}$ involves only the transposition of bond pairs, its effect on loops is limited to splitting one loop into two (when i and j belong to the same loop) and joining two loops into one (when i and j belong to different loops). Its correlation function obeys the simple rule

$$C_{\underbrace{ijkl\ldots}_{2n\text{ indices}}} = \frac{\langle Q|\hat{\gamma}_{ij}\hat{\gamma}_{kl}\cdots|P\rangle}{\langle Q|P\rangle} = 2^{\Delta N_{\circlearrowleft}-n} > 0, \tag{71}$$

where $\Delta N_{\circlearrowleft}$ represents the change in loop number after the loops have been split or joined at (i,j), (k,l), etc. Two examples are given in Fig. 7.

We now introduce a generating function

$$F[a] = \log\langle Q|\exp\left(\sum_{ij} a_{ij}\hat{\gamma}_{ij}\right)|P\rangle. \tag{72}$$

Its diagrammatic expansion in powers of the coupling a_{ij}, shown in Fig. 8, is completely analogous to the Goldstone diagrams familiar from standard many-body theory. (There are only connected diagrams because of the linked-cluster theorem.) The nth order derivatives of F are

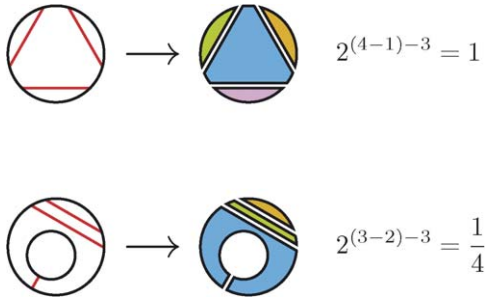

Fig. 7. Two examples of the correlation function defined in Eq. (71) acting at third order.

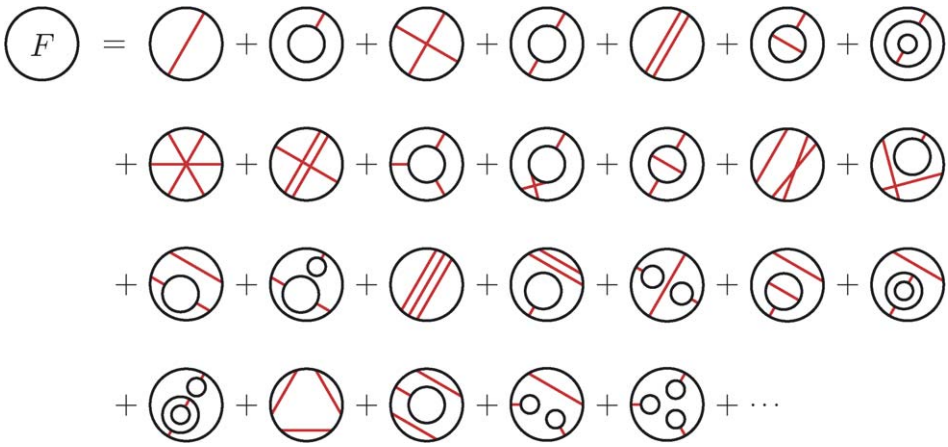

Fig. 8. The diagrammatic expansion of the cumulant generating function F (from Eq. (72)) is shown to third order in the coupling a_{ij}. The black lines denote valence bond loops and the red lines $\hat{\gamma}$ operators.

the cumulants of the correlators defined in Eq. (71),

$$\tilde{C}_{\underbrace{ijk\ldots}_{2n \text{ indices}}} = \left.\frac{\partial^n F}{\partial a_{ij}\partial a_{kl}\cdots}\right|_{a=0}, \tag{73}$$

and are related to them by

$$\tilde{C}_{ij} = C_{ij}, \tag{74}$$

$$\tilde{C}_{ijkl} = C_{ijkl} - \tilde{C}_{ij}\tilde{C}_{kl}, \tag{75}$$

$$\tilde{C}_{ijklmn} = C_{ijklmn} - \tilde{C}_{ij}\tilde{C}_{klmn} - \tilde{C}_{kl}\tilde{C}_{ijmn} - \tilde{C}_{mn}\tilde{C}_{ijkl} - \tilde{C}_{ij}\tilde{C}_{kl}\tilde{C}_{mn}. \tag{76}$$

What is important about the cumulants is that their subtractive terms lead to perfect cancellation (e.g., $C_{ijkl} = C_{ij}C_{kl}$ so that $\tilde{C}_{ijkl} = 0$) whenever the $\hat{\gamma}$-vertices connect the loops into a network that cannot be disentangled by cutting it along two loop segments. The exact statement is that a cumulant vanishes unless its configuration is irreducible in the standard many-body diagram sense. See Fig. 9.

The cumulants, in turn, are related to the physical spin correlation functions by

$$\tilde{C}_{ij} = S_{ijkl} + \frac{1}{4}, \tag{77}$$

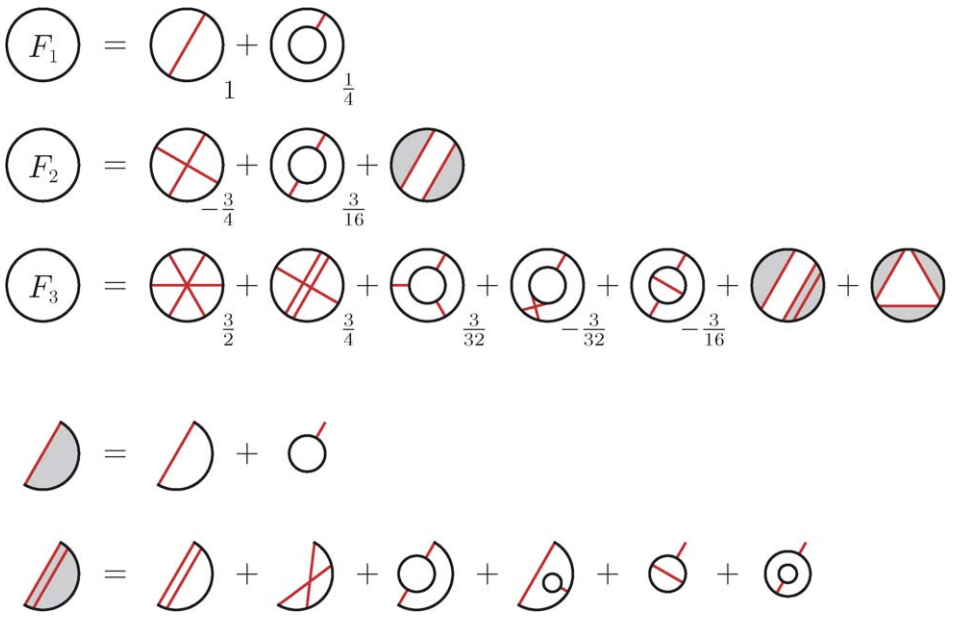

Fig. 9. At each order, the contributions to F can be classified according to their irreducibility. Nonirreducible diagrams are those that can be stitched together from self-energy parts of lower order in $\hat{\gamma}$. The self-energy parts, shown as shaded arcs, are built by removing a single loop segment from the diagrams in Fig. 8. The values listed next to each diagram represent the $\tilde{C}$ cumulant value associated with that configuration. $\tilde{C} = 0$ for the composite terms.

$$\tilde{C}_{ijkl} = S_{ijkl} - S_{ij}S_{kl}, \tag{78}$$

$$\tilde{C}_{ijklmn} = S_{ijklmn} - S_{ij}S_{klmn} - S_{kl}S_{ijmn} - S_{mn}S_{ijkl} + 2S_{ij}S_{kl}S_{mn}. \tag{79}$$

Here, we have used the shorthand

$$S_{ijkl\ldots} = (\epsilon_{ij}\epsilon_{kl}\cdots)\frac{\langle Q|(\mathbf{S}_i\cdot\mathbf{S}_j)(\mathbf{S}_k\cdot\mathbf{S}_l)\cdots|P\rangle}{\langle Q|P\rangle}. \tag{80}$$

Thus, computing spin correlation functions at any order is just a matter of determining the relevant irreducible diagrams, computing the corresponding cumulants, and then solving for the desired term in Eqs. (77)–(79). By this means, we recover the loop estimators Eqs. (56) and (60).

It is also possible to compute even powers of the staggered magnetization by summing over all the site indices:

$$\sum_{ij}\tilde{C}_{ij} = \mathbf{M}_{\mathcal{L}}^2 + N^2, \tag{81}$$

$$\sum_{ijkl}\tilde{C}_{ijkl} = \mathbf{M}_{\mathcal{L}}^4 - \left(\mathbf{M}_{\mathcal{L}}^2\right)^2, \tag{82}$$

$$\sum_{ijklmn}\tilde{C}_{ijklmn} = \mathbf{M}_{\mathcal{L}}^6 - 3\mathbf{M}_{\mathcal{L}}^2\mathbf{M}_{\mathcal{L}}^4 + 2\left(\mathbf{M}_{\mathcal{L}}^2\right)^3. \tag{83}$$

At second order in $\hat{\mathbf{M}}$ (first order in $\hat{\gamma}_{ij}$), there are two irreducible diagrams: a one-loop configuration of weight 1 and a two-loop configuration of weight $1/4$. Since there are L_α^2 ways to select

two sites in loop α and $L_\alpha L_\beta$ ways to select one site in loop α and one in loop β, we have

$$\mathbf{M}_{\mathcal{L}}^2 = 1\sum_\alpha L_\alpha^2 + \frac{1}{4}\sum_{\alpha\neq\beta} L_\alpha L_\beta - N^2 = \frac{3}{4}\sum_\alpha L_\alpha^2 + \frac{1}{4}\Big(\sum_\alpha L_\alpha\Big)^2 - N^2 = \frac{3}{4}\sum_\alpha L_\alpha^2. \quad (84)$$

A glance at Eq. (61) confirms that this method produces the correct result.

At fourth order in $\hat{\mathbf{M}}$ (second order in $\hat{\gamma}_{ij}$), there are again only two irreducible diagrams: a one-loop (cross) configuration of weight $-3/4$ and a two-loop configuration of weight $3/16$. We have already worked out the counting in Eq. (62). Hence,

$$\begin{aligned}\mathbf{M}_{\mathcal{L}}^4 &= -\frac{3}{4}\sum_\alpha\Big(\frac{1}{3}L_\alpha^4 - \frac{4}{3}L_\alpha^2\Big) + \frac{3}{16}\sum_{\alpha\neq\beta} 2L_\alpha^2 L_\beta^2 + \big(\mathbf{M}_{\mathcal{L}}^2\big)^2 \\ &= \sum_\alpha\Big(-\frac{5}{8}L_\alpha^4 + L_\alpha^2\Big) + \frac{3}{8}\Big(\sum_\alpha L_\alpha^2\Big)^2 + \Big(\frac{3}{4}\sum_\alpha L_\alpha^2\Big)^2 \\ &= \sum_\alpha\Big(-\frac{5}{8}L_\alpha^4 + L_\alpha^2\Big) + \frac{15}{16}\Big(\sum_\alpha L_\alpha^2\Big)^2, \end{aligned} \quad (85)$$

which is the result of Eq. (64).

At sixth order in $\hat{\mathbf{M}}$ (third order in $\hat{\gamma}_{ij}$), there are five irreducible diagrams. The diagrams of weight $3/32$ and $-3/32$ both number $\sum_{\alpha\neq\beta} 2L_\alpha^3 L_\beta^3$ and thus cancel each other, so we only need to consider the other three: a one-loop (asterisk) configuration of weight $3/2$, a one-loop (railway tie) configuration of weight $3/4$, and a two-loop configuration of weight $-3/16$. Counting the number of site index arrangements for these three cases requires some work, but it is no different in principle from what we did in Eq. (62). We skip the details and simply report the result:

$$\begin{aligned}\mathbf{M}_{\mathcal{L}}^6 &= \frac{3}{2}\sum_\alpha\Big(\frac{1}{15}L_\alpha^6 - \frac{16}{15}L_\alpha^2\Big) + \frac{3}{4}\sum_\alpha\Big(\frac{1}{5}L_\alpha^6 - \frac{4}{3}L_\alpha^4 + \frac{32}{15}L_\alpha^2\Big) \\ &\quad - \frac{3}{16}2\sum_{\alpha\neq\beta} L_\alpha^2 L_\beta^2\big(L_\alpha^2 + L_\beta^2 - 4\big) + 3\mathbf{M}_{\mathcal{L}}^2\mathbf{M}_{\mathcal{L}}^4 - 2\big(\mathbf{M}_{\mathcal{L}}^2\big)^3. \end{aligned} \quad (86)$$

This simplifies to

$$\mathbf{M}_{\mathcal{L}}^6 = \sum_\alpha\Big(L_\alpha^6 - \frac{5}{2}L_\alpha^4\Big) + \frac{81}{64}\Big(\sum_\alpha L_\alpha^2\Big)^3 - \frac{69}{32}\Big(\sum_\alpha L_\alpha^4\Big)\Big(\sum_\alpha L_\alpha^2\Big). \quad (87)$$

In terms of the $\bar{Q}P$ cycle lengths ($L_\alpha \to 2k_\alpha$), the magnetization formulas are

$$\mathbf{M}_{\mathcal{L}}^2 = 3\sum_\alpha k_\alpha^2, \quad (88)$$

$$\mathbf{M}_{\mathcal{L}}^4 = \sum_\alpha\big(-10k_\alpha^4 + 4k_\alpha^2\big) + 15\Big(\sum_\alpha k_\alpha^2\Big)^2, \quad (89)$$

$$\mathbf{M}_{\mathcal{L}}^6 = \sum_\alpha\big(64k_\alpha^6 - 40k_\alpha^4\big) + 81\Big(\sum_\alpha k_\alpha^2\Big)^3 - 138\Big(\sum_\alpha k_\alpha^4\Big)\Big(\sum_\alpha k_\alpha^2\Big). \quad (90)$$

Recall that in Section 5 we used $n_k = \sum_{\alpha=1}^{N_\circlearrowleft}\delta(k-k_\alpha)$, the cycle length distribution function, to derive an expression for the overlap $\langle Q|P\rangle$. It is easy to see that the second moment of n_k

Table 3
Asymptotic behaviour of the loop density and staggered magnetization in the thermodynamic limit as a function of the loop distribution tail

$\langle n_k\rangle_W \sim k^{-p}$	$\mathcal{O}(\langle N_{\circlearrowleft}\rangle/N)$	$\mathcal{O}(\langle \hat{\mathbf{M}}^2\rangle/N^2)$
$0 \leqslant p < 1$	$\frac{1}{N}$	1
$p = 1$	$\frac{\log N}{N}$	1
$1 < p < 2$	$\frac{1}{N^{2-p}}$	1
$p = 2$	$\frac{1}{\log N}$	$\frac{1}{\log N}$
$2 < p < 3$	1	$\frac{1}{N^{p-2}}$
$p \geqslant 3$	1	$\frac{1}{N}$
short-ranged	1	$\frac{1}{N}$

is related to the presence of long-range antiferromagnetic order in the system: a loop average of Eq. (88) gives $\langle \hat{\mathbf{M}}^2\rangle = \sum_k 3k^2\langle n_k\rangle_W$. Similarly, the fourth and sixth powers of the staggered magnetization have terms involving the cycle-length correlations $\langle n_k n_{k'}\rangle_W$ and $\langle n_k n_{k'} n_{k''}\rangle_W$.

The key feature is the tail of the cycle-length distribution. If it is too weak, then the loop gas is characterized by a macroscopic number of small loops. In the opposite limit, the system has a vanishing number density of loops, although each loop contains a nonvanishing fraction of all the spins. These system-spanning loops are the foundation of the long-range order. As an example, suppose that $\langle n_k\rangle_W \sim k^{-p}$, with the normalization set by the constraint $N = \sum_{k=1}^{N} k\langle n_k\rangle_W$. The standard large-$N$ summation rules are

$$\sum_{k=1}^{N} k^{-p} = \begin{cases} \frac{1}{1-p}N^{1-p} + \mathcal{O}(N^{-p}) & \text{if } p < 1, \\ \log N + \mathcal{O}(1) & \text{if } p = 1, \\ \zeta(p) + \mathcal{O}(N^{1-p}) & \text{if } p > 1, \end{cases} \tag{91}$$

where $\zeta(p)$ is the Riemann zeta function. These can be used to derive the asymptotic behaviour listed in Table 3. Fig. 10 depicts the $N \to \infty$ behaviour of the loop number density and the average staggered moment:

$$\frac{\langle N_{\circlearrowleft}\rangle}{N} = \frac{1}{N}\sum_{k=1}^{N}\langle n_k\rangle_W \to \frac{\zeta(p)}{\zeta(p-1)}\theta(p-2), \tag{92}$$

$$\frac{\langle \hat{\mathbf{M}}^2\rangle}{(2N)^2} = \frac{3}{4N^2}\sum_{k=1}^{N} k^2\langle n_k\rangle_W \to \frac{3(2-p)}{4(3-p)}\theta(2-p). \tag{93}$$

Clearly, long-range order exists for a range of exponents $0 \leqslant p < 2$. The phase transition at the critical value $p_c = 2$ should be visible as a sharp step in the function $\langle \hat{\mathbf{M}}^2\rangle/\langle N_{\circlearrowleft}\rangle^2$ and in the Binder ratios [44] $\langle \hat{\mathbf{M}}^4\rangle/\langle \hat{\mathbf{M}}^2\rangle^2$ and $\langle \hat{\mathbf{M}}^6\rangle/\langle \hat{\mathbf{M}}^2\rangle^3$.

In the $p \to \infty$ limit, the cycle-length distribution becomes sharply peaked at the minimum length, $\langle n_k\rangle_W = N\delta_{k,1}$, which is the result for a fixed dimer configuration. More generally, a generic VBS state will have $\langle n_k\rangle_W \sim \theta(N_0 - k)$, where N_0 is the size of the plaquette (the basic unit of translational symmetry breaking). When the distribution is short-ranged—having either an upper cutoff or an exponentially suppressed tail—there is no magnetic order.

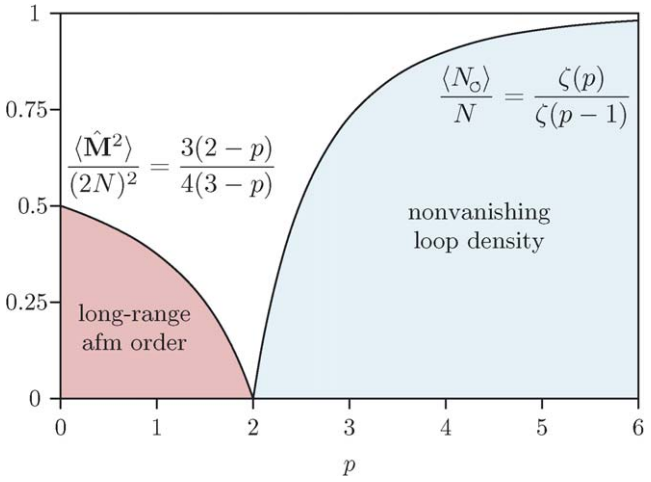

Fig. 10. The squared staggered magnetization and the loop density are plotted as a function of the exponent p for a cycle-length distribution of the form $\langle n_k \rangle_W \sim k^{-p}$. The two quantities are complementary indicators of the long range order below $p = 2$.

8. Valence bond coverings of the full Hilbert space

In previous sections, we discussed the properties of the $S = 0$ valence bond states. We now turn our attention to the full Hilbert space and consider *extended* valence bond states of the form

$$|P; \vec{\mu}\rangle = \prod_{n=1}^{N} \chi^{\mu_n \dagger}_{i_n, P j_n} |\text{vac}\rangle. \tag{94}$$

Here, $\vec{\mu} = (\mu_1, \mu_2, \ldots, \mu_N) \in \mathbb{Z}_4^N$ is a vector of indices describing the singlet/triplet character of each bond. The set of such states is overcomplete with respect to the full Hilbert space ($4^N N! \gg 2^{2N}$). The restriction to AB bonds is still meaningful in the extended basis since for every index pair μ'', ν'' there is at least one set of indices μ, ν, μ', ν' (in fact there are exactly four) such that the equation

$$c_1 \chi^{\mu\dagger}_{il} \chi^{\nu\dagger}_{jk} + c_2 \chi^{\mu'\dagger}_{ij} \chi^{\nu'\dagger}_{kl} + c_3 \chi^{\mu''\dagger}_{lj} \chi^{\nu''\dagger}_{ik} = 0 \tag{95}$$

has a nontrivial solution. This is the singlet/triplet generalization of Eq. (25).

To understand how triplet states evolve under the Heisenberg Hamiltonian, we must reproduce the analysis of Section 4 but now with Eqs. (10) and (22) specialized to

$$\left[\chi^0_{ij}, \chi^{\mu\dagger}_{ij}\right]|\text{vac}\rangle = \delta^{0\mu}|\text{vac}\rangle \tag{96}$$

and

$$\left[\chi^0_{ij}, \chi^{\mu\dagger}_{kj} \chi^{\nu\dagger}_{il}\right]|\text{vac}\rangle = \frac{1}{2} T^{\lambda\mu 0\nu} \chi^{\lambda\dagger}_{kl} |\text{vac}\rangle. \tag{97}$$

As before, the operator $-\hat{H}_{ij}$ has both a diagonal and offdiagonal part. If there is a pre-existing singlet bond across the active sites, the bond configuration is left unchanged. If there is a pre-existing triplet bond, however, the state is annihilated. Otherwise, the bonds are rearranged and the singlet/triplet labels reassigned in a spin-conserving fashion. The update rule for $-\hat{H}_{ij}$ with

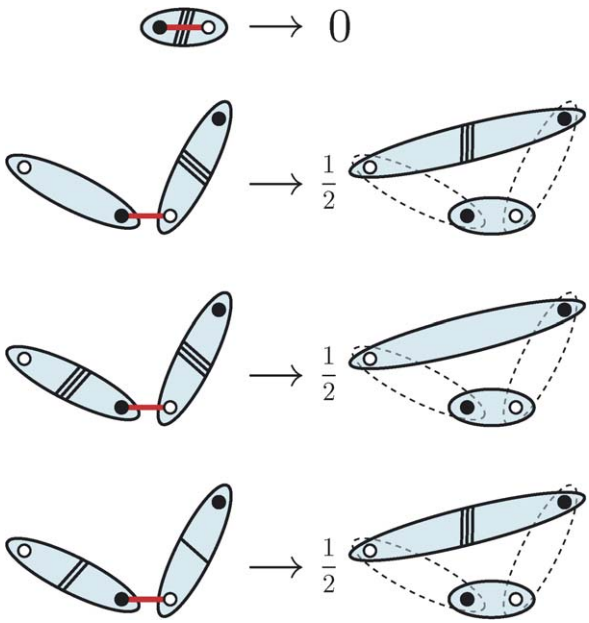

Fig. 11. Summary of the update rules for triplet bonds. The number of cross hatches on each bond indicates its triplet character.

$i \in A$ and $j \in B$, illustrated in Fig. 11, is given by

$$-\hat{H}_{i_n j_m}|P;\vec{\mu}\rangle = \begin{cases} \delta^{\mu_n 0}|P;\vec{\mu}\rangle & \text{if } Pm = n, \\ \frac{1}{2}T^{\lambda\mu_n 0\mu_{\bar{P}m}}|(Pn\ m)P;\vec{\mu}'\rangle & \text{otherwise} \end{cases} \tag{98}$$

with

$$\vec{\mu}' = (\mu_1, \ldots, \mu_{n-1}, 0, \mu_{n+1}, \ldots, \mu_{\bar{P}m-1}, \lambda, \mu_{\bar{P}m+1}, \ldots, \mu_N). \tag{99}$$

There are some important differences from the purely singlet-bond case. There is now the possibility of annihilating a state by acting directly on a triplet bond, unlike in the singlet sector, where $(\hat{H}_{ij}\hat{H}_{i'j'}\hat{H}_{i''j''}\cdots)|P\rangle \neq 0$ always. Also, when bonds of different species interact, the weight $T^{\lambda\mu 0\nu}$ is potentially negative: the τ operators obey the identity

$$\tau^{\mu}\tau^{0\dagger}\tau^{\nu} = \begin{pmatrix} \tau^0 & \tau^1 & \tau^2 & \tau^3 \\ \tau^1 & \tau^0 & \tau^3 & -\tau^2 \\ \tau^2 & -\tau^3 & \tau^0 & \tau^1 \\ \tau^3 & \tau^2 & -\tau^1 & \tau^0 \end{pmatrix}_{\mu\nu} \tag{100}$$

and hence

$$T^{\lambda\mu 0\nu} = \delta^{\lambda 0}\delta^{\mu\nu} + \epsilon^{\mu\nu\lambda}, \tag{101}$$

where $\epsilon^{\mu\nu\lambda}$ is the alternating symbol.

Overlaps of extended valence bond states can be computed as before, only now we must use the most general form of the anticommutation relationship in Eq. (22). We find that

$$\langle Q;\vec{\nu}|P;\vec{\mu}\rangle = 2^{N_{\circlearrowleft}-N}\prod_{\alpha=1}^{N_{\circlearrowleft}} K_{\alpha}. \tag{102}$$

Here, $N_{\circlearrowleft}$ is the number of cycles in $\bar{Q}P$ and K_α is a chirality factor whose value is given by the trace of the product of $\tau^{\nu_n\dagger}\tau^{\mu_n}$ in proper order around each cycle. The form of K_α follows from the "boxcar" property

$$\sum_\lambda \mathrm{tr}\big(\cdots\tau^{\nu\dagger}\tau^{\lambda}\big)T^{\lambda\mu\nu'\mu'} = \mathrm{tr}\big(\cdots\tau^{\nu\dagger}\tau^{\mu}\tau^{\nu'\dagger}\tau^{\mu'}\big). \tag{103}$$

For example, the loop $\bar{Q}P = (1\,2\,4\,5\,3)\cdots$, highlighted in Fig. 4, has associated with it a factor

$$K_\alpha = \frac{1}{2}\,\mathrm{tr}\big(\tau^{\nu_1\dagger}\tau^{\mu_1}\tau^{\nu_2\dagger}\tau^{\mu_2}\tau^{\nu_4\dagger}\tau^{\mu_4}\tau^{\nu_5\dagger}\tau^{\mu_5}\tau^{\nu_3\dagger}\tau^{\mu_3}\big). \tag{104}$$

Since K_α takes the values 0 or ±1, the overlap is no longer guaranteed to be positive definite, as it was in the case of only singlet bonds. If we do not mix triplet species, however, positive definiteness is preserved. In that case, $K_\alpha = 1$ if the loop contains an even number of triplets and $K_\alpha = 0$ if the loop contains an odd number. More generally, if we move around a given loop in proper order, encountering triplets of species $a, b, c, \ldots$ along the way, then K_α takes the value

$$\begin{aligned}
&0 && \text{one triplet,}\\
&(-1)^{1+|\vec{\mu}|}\delta^{ab} && \text{two triplets,}\\
&(-1)^{1+|\vec{\mu}|}\epsilon^{abc} && \text{three triplets,}\\
&(-1)^{|\vec{\mu}|}\big(\delta^{ab}\delta^{cd}+\delta^{ad}\delta^{bc}-\delta^{ac}\delta^{bd}\big) && \text{four triplets,}
\end{aligned} \tag{105}$$

where $|\vec{\mu}|$ counts the number of nonzero entries (triplets) in $\vec{\mu}$ that belong to the loop in question. In other words, the overall sign depends on how many triplets arise from $|P;\vec{\mu}\rangle$ and how many from $|Q;\vec{\nu}\rangle$.

9. Staggered magnetization components

The staggered magnetization operator has the special property that it can always be written so as to induce no rearrangement of bonds. This is simply a matter of grouping its terms to match the particular bond tiling of the state it is acting on. That is, for any $P \in \mathcal{S}_N$,

$$\hat{M}^a = \sum_{i\in A} S^a_i - \sum_{j\in B} S^a_j = \sum_{n=1}^{N}\big(S^a_{i_n} - S^a_{j_{Pn}}\big). \tag{106}$$

Since the bracketed term behaves according to Eq. (13), we see that the effect of $\hat{M}^a$ on an $S=0$ valence bond state is to create a superposition of states, each of which has one bond promoted to an a-triplet:

$$\hat{M}^a|P\rangle = i\sum_{n=1}^{N}|P;a_n\rangle. \tag{107}$$

Here, $|P;a_n\rangle$ denotes the state $|P;\vec{\mu}\rangle$ with $\vec{\mu}$ having all zero entries except for a in the nth slot. Since lone triplets always produce zero-contribution loops, we find that

$$M^a_{\mathcal{L}} = \frac{\langle Q|\hat{M}^a|P\rangle}{\langle Q|P\rangle} = i\sum_{n=1}^{N}\frac{\langle Q|P;a_n\rangle}{\langle Q|P\rangle} = 0, \tag{108}$$

which is the expected result for rotationally invariant states $|P\rangle$ and $|Q\rangle$. Two triplets of the same species, however, if they originate in different states, give unit weight whenever they lie in the same loop. Thus,

$$\left(M^a M^b\right)_{\mathcal{L}} = \sum_{m=1}^{N}\sum_{n=1}^{N} \frac{\langle Q; a_m | P; b_n\rangle}{\langle Q|P\rangle} = \delta^{ab}\sum_{\alpha} k_\alpha^2. \tag{109}$$

The final equality holds because, in a cycle of length k_α, there are k_α ways to place the mth Q link and k_α ways to place the nth P link.

Correlation functions at fourth order can be computed in much the same way. Two applications of $\hat{M}^a$ to a valence bond state yields

$$\left(\hat{M}^a\right)^2|P\rangle = N|P\rangle - \sum_{m\neq n}|P; a_m, a_n\rangle, \tag{110}$$

and the overlap of two such states is

$$\begin{aligned}\frac{\langle Q|(\hat{M}^a)^2(\hat{M}^b)^2|P\rangle}{\langle Q|P\rangle} &= N^2 - \sum_{m\neq n}\left(\frac{\langle Q; a_m, a_n|P\rangle}{\langle Q|P\rangle} + \frac{\langle Q|P; b_m, b_n\rangle}{\langle Q|P\rangle}\right) \\ &\quad + \sum_{m\neq n}\sum_{m'\neq n'}\frac{\langle Q; a_m, a_n|P; b_{m'}, b_{n'}\rangle}{\langle Q|P\rangle}.\end{aligned} \tag{111}$$

The bracketed terms in Eq. (111) each take the value -1 if the two triplets are in the same loop and vanish otherwise. In the case of one triplet species ($a = b$), the final term contributes if there is either a single loop containing all four triplets or a pair of loops containing two triplets each. These configurations all have weight $+1$. Applying the appropriate counting arguments yields

$$\begin{aligned}\left(M^a\right)^4_{\mathcal{L}} &= N^2 + 2N\sum_{\alpha} k_\alpha(k_\alpha - 1) + \sum_{\alpha} k_\alpha^2(k_\alpha - 1)^2 \\ &\quad + \sum_{\alpha\neq\beta} k_\alpha(k_\alpha - 1)k_\beta(k_\beta - 1) + 2\sum_{\alpha\neq\beta} k_\alpha^2 k_\beta^2.\end{aligned} \tag{112}$$

Note that the $m \neq n$ and $m' \neq n'$ constraints have no effect when m and m' (m and n') are in one cycle and n and n' (n and m') are in another. Eq. (112) simplifies considerably to give

$$\left(M^a\right)^4_{\mathcal{L}} = -2\sum_{\alpha} k_\alpha^4 + 3\left(\sum_{\alpha} k_\alpha^2\right)^2. \tag{113}$$

If there are two triplet species ($a \neq b$), the situation is slightly more complicated. When all four triplets are in the same loop, there are

$$2k_\alpha\sum_{n=3}^{k_\alpha}(n-1)(n-2) = \frac{2}{3}k_\alpha^4 - 2k_\alpha^3 + \frac{4}{3}k_\alpha^2 \tag{114}$$

configurations, having weight $+1$, in which the a and b triplets appear in consecutive order around the loop ($aabb$) and

$$2k_\alpha\sum_{n=2}^{k_\alpha}(n-1)(k-n+1) = -\frac{1}{3}k_\alpha^2 + \frac{1}{3}k_\alpha^4 \tag{115}$$

configurations, having weight -1, in which they appear in alternating order $(abab)$. (Note that Eqs. (114) and (115) sum to $k_\alpha^2(k_\alpha-1)^2$, as required.) There is also a positive contribution when the a and b triplets are paired $(aa)(bb)$ in two different loops, but none when they are paired $(ab)(ab)$. Hence,

$$\begin{aligned}\left[\left(M^a\right)^2\left(M^b\right)^2\right]_{\mathcal{L}} &= N^2 + 2N\sum_\alpha k_\alpha(k_\alpha-1) + \sum_\alpha\left(\frac{2}{3}k_\alpha^4 - 2k_\alpha^3 + \frac{4}{3}k_\alpha^2\right)\\ &\quad - \sum_\alpha\left(\frac{1}{3}k_\alpha^4 - \frac{1}{3}k_\alpha^2\right) + \sum_{\alpha\neq\beta} k_\alpha(k_\alpha-1)k_\beta(k_\beta-1),\end{aligned} \tag{116}$$

which simplifies to

$$\left[\left(M^a\right)^2\left(M^b\right)^2\right]_{\mathcal{L}} = \sum_\alpha\left(\frac{2}{3}k_\alpha^2 - \frac{2}{3}k_\alpha^4\right) + \left(\sum_\alpha k_\alpha^2\right)^2. \tag{117}$$

It is important to verify that these expressions are compatible with those of Sections 6 and 7. First, spin isotropy demands that $\langle(\hat{M}^a)^2\rangle = \frac{1}{3}\langle\hat{\mathbf{M}}^2\rangle$, which is confirmed by comparing Eqs. (88) and (109). Second, the identity

$$\hat{\mathbf{M}}^4 = \sum_a\left(\hat{M}^a\right)^4 + \sum_{a\neq b}\left(\hat{M}^a\right)^2\left(\hat{M}^b\right)^2 \tag{118}$$

requires that $3\times$ Eq. (113) and $6\times$ Eq. (117) sum to Eq. (89), which is indeed true. In summary, the loops estimators for components of the staggered magnetization at second and fourth order are

$$\left(M^aM^b\right)_{\mathcal{L}} = \delta^{ab}\sum_\alpha k_\alpha^2, \tag{119}$$

$$\left[\left(M^a\right)^2\left(M^b\right)^2\right]_{\mathcal{L}} = \frac{2}{3}\sum_\alpha\left[\left(1-\delta^{ab}\right)k_\alpha^2 - \left(1+2\delta^{ab}\right)k_\alpha^4\right] + \left(1+2\delta^{ab}\right)\left(\sum_\alpha k_\alpha^2\right)^2. \tag{120}$$

10. The Néel state

For a bipartite spin system, in which the A and B site labels designate genuine sublattices, the Néel state can be written in terms of any AB valence bond configuration. This freedom exists because the staggered moments can be organized into spin-up/spin-down pairs such that

$$|R\rangle = \prod_{i\in A} b_{i\uparrow}^\dagger \prod_{j\in B} b_{j\downarrow}^\dagger|\text{vac}\rangle = \prod_{n=1}^N b_{i_n\uparrow}^\dagger b_{j_{Pn}\downarrow}^\dagger|\text{vac}\rangle \tag{121}$$

for any $P\in\mathcal{S}_N$. Since $b_{i\uparrow}^\dagger b_{j\downarrow}^\dagger = \frac{1}{\sqrt{2}}(\chi_{ij}^{0\dagger} + i\chi_{ij}^{3\dagger})$, the Néel state can be viewed as a superposition of states with a fixed (but arbitrary) bond configuration and total triplet number ranging from 0 to N:

$$|R\rangle = \frac{1}{2^{N/2}}\left[|P\rangle + i\sum_{n=1}^N|P;3_n\rangle - \sum_{m<n}|P;3_m,3_n\rangle + \cdots\right]. \tag{122}$$

If we define $t_a(\vec{\mu}) = \sum_{n=1}^{N} \delta_{\mu_n,a}$, which counts the number of a-triplets in the index vector $\vec{\mu}$, then the overlap of $|R\rangle$ with an extended valence bond state $|P;\vec{\mu}\rangle$ can be written as

$$\langle R|P;\vec{\mu}\rangle = \delta_{t_1,0}\delta_{t_2,0}e^{i(\pi/2)t_3}2^{-N/2}. \tag{123}$$

The overlap vanishes if the state $|P;\vec{\mu}\rangle$ contains any 1- or 2-triplets. Otherwise it is independent of P and constant up to an overall phase factor with an angle given by $\pi/2 \times$ the number of 3-triplets. The derivation of Eq. (123) relies on nothing more than the (species) orthogonality of bonds that connect the same two sites (expressed in Eq. (10)). There is no need to account for bond-configurational mismatch because the permutation P in Eq. (122) can be chosen equal to the permutation in $|P;\vec{\mu}\rangle$.

Matrix elements taken between the Néel state and a valence bond singlet state are particularly easy to compute. For example, applying Eq. (68), we find that

$$\frac{\langle R|\hat{\gamma}_{i_n j_m}|P\rangle}{\langle R|P\rangle} = \left(\frac{1}{2}\right)^{1-\delta_{Pn,m}} \frac{\langle R|(Pn\ m)P\rangle}{\langle R|P\rangle}, \tag{124}$$

where the ratio of overlaps on the right-hand side is 1 since both $\langle R|P\rangle$ and $\langle R|(Pn\ m)P\rangle$ have the value $2^{-N/2}$. In general, the matrix element picks up a factor of $\frac{1}{2}$ for each offdiagonal $\hat{\gamma}$ operation (keeping in mind that subsequent operations act on the reconfigured bonds). The evaluation rule can be expressed as

$$\frac{\langle R|\overbrace{\hat{\gamma}_{ij}\hat{\gamma}_{kl}\cdots}^{n\text{ operators}}|P\rangle}{\langle R|P\rangle} = 2^{N_{\circlearrowleft}-n}, \tag{125}$$

where $N_{\circlearrowleft}$ now refers to the number of closed loops that are formed by the bonds and $\hat{\gamma}$ vertices.

In analogy with Eq. (102), the rules can be extended to cover states with arbitrary numbers of triplets:

$$\frac{\langle R|\overbrace{\hat{\gamma}_{ij}\hat{\gamma}_{kl}\cdots}^{n\text{ operators}}|P;\vec{\mu}\rangle}{\langle R|P\rangle} = 2^{N_{\circlearrowleft}-n}\prod_{\alpha=1}^{N_{\circlearrowleft}+N_{\leftrightarrow\!\!\!\!\!\!\rho}} K_\alpha. \tag{126}$$

In this case, the index α ranges over both the closed loops and the open strings ($N_{\leftrightarrow\!\!\!\!\!\!\rho}$ in number) that are formed. A closed loop involving $k \leqslant n$ operators and bonds numbered $1, 2, \ldots, k$ has associated with it a factor

$$K_\alpha = \frac{1}{2}\operatorname{tr}\bigl(\tau^{0\dagger}\tau^{\mu_1}\tau^{0\dagger}\tau^{\mu_2}\cdots\tau^{0\dagger}\tau^{\mu_k}\bigr). \tag{127}$$

An open string involving $k \leqslant n$ operators and bonds numbered $1, 2, \ldots, k+1$ has a factor

$$K_\alpha = \frac{i}{2}\operatorname{tr}\bigl(\tau^{3\dagger}\tau^{\mu_1}\tau^{0\dagger}\tau^{\mu_2}\cdots\tau^{0\dagger}\tau^{\mu_{k+1}}\bigr). \tag{128}$$

Note that any lone triplet in a closed loop gives $K_\alpha = 0$, whereas a lone 3-triplet in an open string gives $K_\alpha = i$. See Fig. 12.

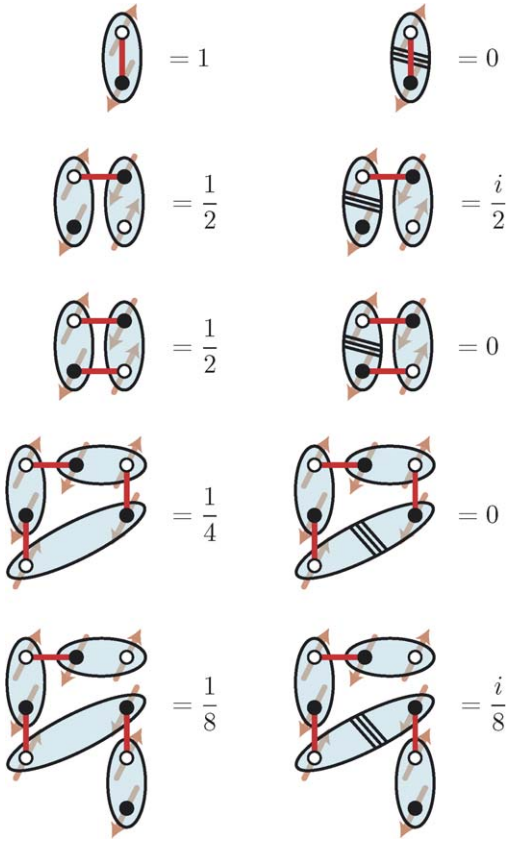

Fig. 12. Matrix elements of $\hat{\gamma}$ taken between a valence bond state and the reference Néel state. Closed loops containing one triplet do not contribute, whereas open strings with one triplet contribute the same value as their singlet-bond-only counterpart.

11. Singlet–triplet gap

Consider a quantum spin system whose Hamiltonian $\hat{H}$ has a global singlet ground state $|\psi_0\rangle$. Starting from an arbitrary singlet trial state

$$\left|\psi_0^{\text{trial}}\right\rangle = \sum_P c_P^{\text{trial}} |P\rangle, \tag{129}$$

the true ground state wavefunction can be obtained by projection:

$$|\psi_0\rangle = \lim_{\tau\to\infty} e^{-\tau\hat{H}} \left|\psi_0^{\text{trial}}\right\rangle = \sum_P c_P |P\rangle. \tag{130}$$

From the eigenequation $\hat{H}|\psi_0\rangle = E_0|\psi_0\rangle$, the ground state energy can be isolated by acting from the left with an appropriate reference state:

$$E_0 = \frac{\langle R|\hat{H}|\psi_0\rangle}{\langle R|\psi_0\rangle}. \tag{131}$$

For our purposes, it is most convenient to use a Néel reference state $|R\rangle$, since it has a constant-magnitude overlap with all states in the full Hilbert space. Thus,

$$E_0 = \frac{\langle R|\hat{H}|\psi_0\rangle}{\langle R|\psi_0\rangle} = \frac{\sum_P W(P)\frac{\langle R|\hat{H}|P\rangle}{\langle R|P\rangle}}{\sum_P W(P)} \tag{132}$$

with $W(P) = c_P\langle R|P\rangle = 2^{-N/2}c_P$. This formulation is similar to that of Eq. (55), except that here the basic objects of interest are bonds rather than loops. We can view the ground state energy $E_0 = \langle H_{\mathcal{B}}\rangle_W$ as the expectation value of the bond estimator for the Hamiltonian, $H_{\mathcal{B}}$, in a fluctuating gas of valence bonds.

Similarly, by constructing a trial wavefunction in the triplet sector,

$$\big|\psi_1^{\text{trial}}\big\rangle = \hat{M}^3\big|\psi_0^{\text{trial}}\big\rangle = i\sum_{n=1}^{N}\sum_P c_P^{\text{trial}}|P;3_n\rangle, \tag{133}$$

we can project onto the lowest-energy triplet state:

$$|\psi_1\rangle = \lim_{\tau\to\infty} e^{-\tau\hat{H}}\hat{M}^3\big|\psi_0^{\text{trial}}\big\rangle. \tag{134}$$

The structure of this projection is closely related to that of Eq. (130). In the singlet case, the evolution operator consists of a long string of $-\hat{H}_{ij}$ operators that successively reconfigure the bond configuration $|P\rangle$ of the trial state. Here, we simply need to compute the result of the same strings operating on $|P;3_n\rangle$. We know, however, that the update rules for singlet and triplet bonds are identical except that a direct diagonal operation kills a triplet. It is straightforward to reinterpret the operator string by designating one bond of the trial state as a triplet and tracing its evolution. As shown in Fig. 13, the triplet will either run the gauntlet or die in the attempt. Accordingly, we can write

$$|\psi_1\rangle = i\sum_{n=1}^{N}\sum_P g_n(P)c_P|P;3_n\rangle, \tag{135}$$

where $g_n(P)$ counts the number of surviving triplets whose final destination is the nth bond of configuration P. By definition,

$$0 \leqslant \sum_{n=1}^{N} g_n(P) \leqslant N. \tag{136}$$

The energy of the low-lying triplet state is

$$E_1 = \frac{\langle R|\hat{H}|\psi_1\rangle}{\langle R|\psi_1\rangle} = \frac{\sum_P W(P)\sum_{n=1}^{N} g_n(P)\frac{\langle R|\hat{H}|P;3_n\rangle}{\langle R|P;3_n\rangle}}{\sum_P W(P)\sum_{n=1}^{N} g_n(P)}. \tag{137}$$

Here we have made use of the fact that $\langle R|P;3_n\rangle = i\langle R|P\rangle$. Alternatively, E_1 can be expressed as

$$E_1 = \frac{\langle\sum_n g_n H_{\mathcal{B}}\rangle_W}{\langle\sum_n g_n\rangle_W} \tag{138}$$

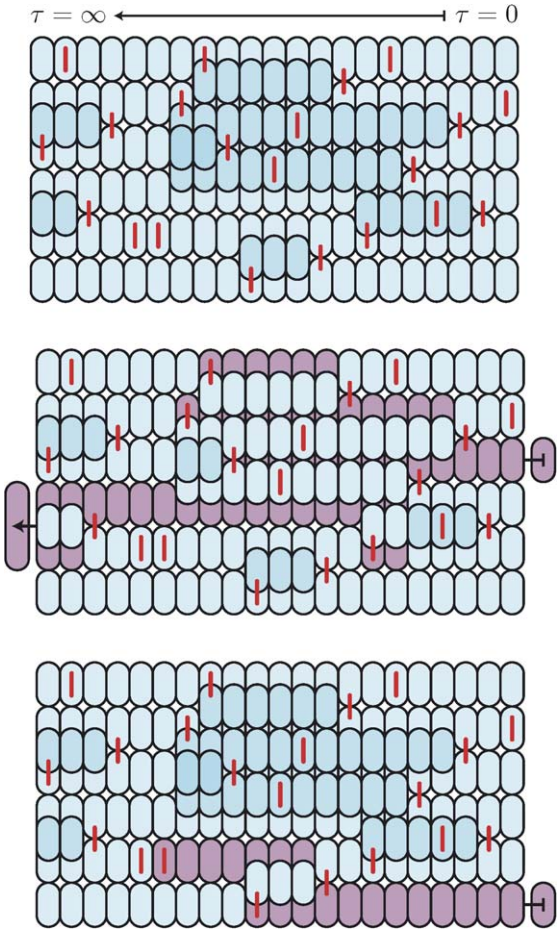

Fig. 13. (Top) The evolution operator (in series expansion) involves long series of $-\hat{H}_{ij}$ operator strings that map VB configurations in the trial state to VB configurations in the true ground state through sequential reordering of the bonds. In the figure, the propagation index [45] increases from right to left along the horizontal axis. A set of singlet valence bonds are arranged along the vertical spatial axis. The red bars denote nearest neighbour interactions. (Middle) The same operator string can be reinterpreted as acting on a trial state with one triplet, marked here in purple. (Bottom) A triplet state that is acted on directly by a diagonal operation is annihilated.

since $\langle R|\hat{H}|P;3_n\rangle/\langle R|P;3_n\rangle$ and $\langle R|\hat{H}|P\rangle/\langle R|P\rangle$ differ only when $g_n = 0$. Combining Eqs. (132) and (138) gives

$$E_1 - E_0 = \frac{\langle \sum_n g_n H_{\mathcal{B}}\rangle_W - \langle \sum_n g_n\rangle_W \langle H_{\mathcal{B}}\rangle_W}{\langle \sum_n g_n\rangle_W}. \tag{139}$$

A numerical measurement of the singlet–triplet gap via Eq. (139) has the advantage that it can be carried out during a simulation of the $S = 0$ ground state properties. This gives a substantial error cancellation in stochastic methods over techniques where E_0 and E_1 are computed individually and subtracted. In some systems, however, the lowest-energy singlet and triplet states may differ so substantially that the reweighting of the operator string becomes inefficient. In that case, so few triplets survive the projection that $\langle \sum_n g_n\rangle \approx 0$.

12. Spin stiffness

Again, let us imagine that the $S = 0$ ground state is obtained via projection:

$$|\psi\rangle = \lim_{\tau\to\infty} e^{-\tau\hat{H}}\big|\psi^{\text{trial}}\big\rangle. \tag{140}$$

Now suppose that we introduce a twist field $\phi(\mathbf{r})$ representing a local rotation of the spins about the 3 axis. We will be concerned with the limit in which the field gradient $\nabla\phi(\mathbf{r})$ is small with respect to the lattice spacing. For concreteness, we endow the field with a single long-wavelength mode $\phi(\mathbf{r}) = \phi_0 + \mathbf{r}\cdot\mathbf{q}$. As a consequence, the relative spin rotation angles satisfy $\theta_{ij} = (\mathbf{r}_i - \mathbf{r}_j)\cdot\mathbf{q}$.

Eq. (20) then suggests that the Hamiltonian—assuming it has the form of Eq. (30)—transforms as

$$-\hat{H} \to -\hat{H}[\mathbf{q}] = -\hat{H} + q^a\hat{T}^a + \frac{1}{2}q^a q^b\hat{G}^{ab}, \tag{141}$$

where the gradient and Hessian are given by

$$\hat{T}^a = \frac{1}{2}\sum_{\langle ij\rangle} J_{ij}(\mathbf{r}_i - \mathbf{r}_j)\cdot\mathbf{e}^a\big(\chi^{0\dagger}_{ij}\chi^3_{ij} + \chi^{3\dagger}_{ij}\chi^0_{ij}\big) + \cdots \tag{142}$$

and

$$\hat{G}^{ab} = \frac{1}{2}\sum_{\langle ij\rangle} J_{ij}(\mathbf{r}_i - \mathbf{r}_j)\cdot\mathbf{e}^a(\mathbf{r}_i - \mathbf{r}_j)\cdot\mathbf{e}^b\big(-\chi^{0\dagger}_{ij}\chi^0_{ij} + \chi^{3\dagger}_{ij}\chi^3_{ij}\big) + \cdots. \tag{143}$$

Here, $+\cdots$ represents additional interaction terms in K_{ijkl} and beyond. Eq. (142) is a spin current operator that changes the number of triplet bonds by ± 1. (See Fig. 14.) It does so in proportion to the interaction strength and the projection of the bond length onto the axis of propagation. Eq. (143), on the other hand, changes the triplet count by 0 or ± 2.

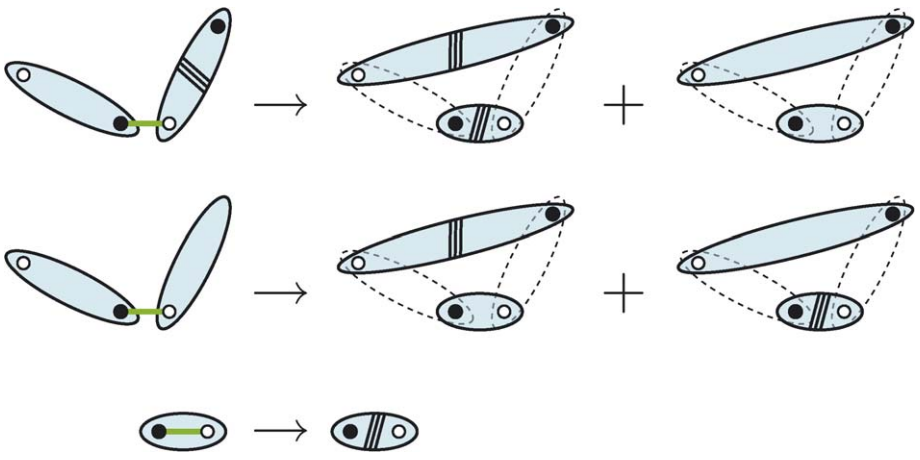

Fig. 14. Several possible bond reconfigurations are shown, corresponding to action by each term in $\hat{T}^a$. The relevant prefactors are suppressed.

Under the influence of the twist field, the ground state energy is

$$E[\mathbf{q}] = \lim_{\tau\to\infty} \frac{\langle R|\hat{H}[\mathbf{q}]e^{-\tau\hat{H}[\mathbf{q}]}|\psi_0\rangle}{\langle R|e^{-\tau\hat{H}[\mathbf{q}]}|\psi_0\rangle}. \tag{144}$$

By virtue of the variational principle, $E[\mathbf{q}]$ must be stationary with respect to variation. Its convexity at $\mathbf{q}=0$ is a measure of the spin stiffness. Derivatives $\partial_a = \partial/\partial q^a$ can be handled using the identity

$$\int_0^\tau d\tau'\, e^{-(\tau-\tau')\hat{H}}\partial_a\hat{H}e^{-\tau'\hat{H}} = -\partial_a\big(e^{-\tau\hat{H}}\big). \tag{145}$$

Hence,

$$\left.\frac{\partial E[\mathbf{q}]}{\partial q^a}\right|_{\mathbf{q}=0} = \frac{\langle R|\hat{T}^a|\psi\rangle}{\langle R|\psi\rangle} + \frac{\langle R|(\hat{H}-E)|\psi^a\rangle}{\langle R|\psi\rangle} = 0, \tag{146}$$

with $|\psi^a\rangle = \partial_a|\psi\rangle|_{\mathbf{q}=0}$ given by

$$\big|\psi^a\big\rangle = \int_0^\tau d\tau'\, e^{-(\tau-\tau')\hat{H}}\hat{T}^a e^{-\tau'\hat{H}}\big|\psi^{\text{trial}}\big\rangle. \tag{147}$$

The state $|\psi^a\rangle$ evolves from the singlet trial state but differs from the projected ground state in that it is constructed with an $\mathbf{e}^a$-directed triplet injected at all times $\tau' < \tau$.

Making use of Eq. (146), we can show that the spin stiffness is given by

$$\rho_{\text{S}}^{ab} = \left.\frac{\partial^2 E[\mathbf{q}]}{\partial q^a\partial q^b}\right|_{\mathbf{q}=0} = \frac{\langle R|\hat{G}^{ab}|\psi\rangle}{\langle R|\psi\rangle} + \frac{\langle R|\hat{T}^a|\psi^b\rangle}{\langle R|\psi\rangle} + \frac{\langle R|\hat{T}^b|\psi^a\rangle}{\langle R|\psi\rangle} + \frac{\langle R|(\hat{H}-E)|\psi^{ab}\rangle}{\langle R|\psi\rangle}, \tag{148}$$

where

$$\begin{aligned}\big|\psi^{ab}\big\rangle = {}& \int_0^\tau d\tau' \int_{\tau'}^\tau d\tau''\, e^{-(\tau-\tau'')\hat{H}}\hat{T}^a e^{-(\tau''-\tau')\hat{H}}\hat{T}^b e^{-\tau'\hat{H}}\big|\psi^{\text{trial}}\big\rangle \\ & + \int_0^\tau d\tau' \int_{\tau'}^\tau d\tau''\, e^{-(\tau-\tau'')\hat{H}}\hat{T}^b e^{-(\tau''-\tau')\hat{H}}\hat{T}^a e^{-\tau'\hat{H}}\big|\psi^{\text{trial}}\big\rangle \\ & + \int_0^\tau d\tau'\, e^{-(\tau-\tau')\hat{H}}\hat{G}^{ab}e^{-\tau'\hat{H}}\big|\psi^{\text{trial}}\big\rangle.\end{aligned} \tag{149}$$

The state $|\psi^{ab}\rangle$ evolves from the singlet trial state $|\psi^{\text{trial}}\rangle$ with two $\mathbf{e}^a$- and $\mathbf{e}^b$-directed triplets injected at times τ' and τ''.

Eq. (148) can be evaluated using the reweighting trick introduced in Section 11. The same operator sequence used to generate the singlet ground state can be reinterpreted to include all possible triplet pairs (at all possible starting locations, not simply at the $\tau = 0$ end as was the case for the singlet–triplet gap measurement). The spin stiffness is related to the fluctuations in energy of the final bond configuration arising from operator sequences in which neither triplet is annihilated.

13. Summary

We have presented in detail a formal framework for organizing calculations in the valence bond basis. This approach is based on manipulations of valence bond creation and annihilation operators, $\chi_{ij}^{\mu\dagger}$ and χ_{ij}^{μ}, that act between any two sites of the spin lattice. These operators are similar to those introduced in Ref. [38] for fixed dimer configurations but are endowed with an expanded operator algebra that is compatible with the overcomplete basis of all possible dimer configurations.

We have focused on what we call the AB valence bond basis, in which half the lattice sites are assigned the label A and the other half B and only dimers connecting sites with different labels are allowed. (The use of AB bonds only is routine in the literature, especially when the Hamiltonian of interest does not contain explicitly frustrating AA/BB interactions.) The states in this restricted basis are uniquely characterized by permutations of the B site labels. Overlaps and matrix elements of such states are related in a systematic way to the cycle structure of the permutations. We have shown, for example, that the presence of antiferromagnetism in a bipartite system is related to the long tail behaviour of the cycle length distribution $\langle n_k \rangle_W$.

Correlation functions of the isotropic spin interaction $\mathbf{S}_i \cdot \mathbf{S}_j$ are related to the cumulants of the operator $\hat{\gamma}_{ij} = \frac{1}{4}(1+\epsilon_{ij}) - \epsilon_{ij}\chi_{ij}^{0\dagger}\chi_{ij}^{0}$. The various contributions can thus be computed in a straightforward way from the set of connected Goldstone diagrams—albeit with the diagrams interpreted quite differently than they are in the usual quantum many-body physics context. (Moreover, there is no need to worry about which of i and j are A or B sites. The different cases are all handled automatically by the sign factor ϵ_{ij}.) As an example of this approach, we have derived explicit expressions for second-, fourth-, and sixth-order expectation values of the staggered magnetization.

We have also emphasized that, when triplet bonds are fully accounted for, the valence bond basis spans the entire Hilbert space, not merely the $S = 0$ subspace. The valence bond operators carry an index μ that specifies the singlet ($\mu = 0$) or triplet ($\mu = 1, 2, 3$) nature of each bond. We have extended the rules for computing overlaps and matrix elements to include states with triplet bonds. As an example of how this can be useful, we have derived expressions for the singet–triplet gap and the spin stiffness that can be interpreted as reweightings of the operator string in a projected singlet ground state. The reweighting formulation is ideally suited for use in valence bond projector Monte Carlo.

Acknowledgement

This work was supported by the National Science Foundation under Grant No. DMR-0513930.

Appendix A

A permutation $P \in \mathcal{S}_N$ is a bijective map that takes n to Pn (and $\bar{P}n$ to n) for every $1 \leqslant n \leqslant N$:

$$P = \begin{pmatrix} 1 & P1 \\ 2 & P2 \\ \vdots & \vdots \\ N & PN \end{pmatrix}. \tag{A.1}$$

An alternative notation for Eq. (A.1) involves cycles of the form (1 2 3), which expresses the functional relationship $1 \to 2$, $2 \to 3$, and $3 \to 1$. Every permutation can be decomposed into a product of disjoint cycles

$$P = \prod_{\alpha=1}^{\#(P)} \left(\xi_\alpha \; P\xi_\alpha \; P^2\xi_\alpha \; \cdots \; P^{k_\alpha - 1}\xi_\alpha\right), \tag{A.2}$$

where $\#(P)$ is the number of cycles in P, ξ_α is a representative number (the lowest, say) in a particular cycle, and k_α is its length. Two numbers n and m are in the same cycle of P iff there is some integer power $k \geqslant 0$ such that $P^k n = m$, which we denote $n \overset{P}{\sim} m$. It follows that n is in the cycle labeled α iff $n \overset{P}{\sim} \xi_\alpha$.

The cycle decomposition given in Eq. (A.2) is unique and requires the fewest possible number of cycles. One can, however, further decompose each term into several smaller cycles that are no longer disjoint (i.e., they may have elements in common). This process can always be carried further until the permutation is expressed entirely as a product of transpositions (cycles of length 2). Accordingly, to understand how the cycle structure of $\bar{Q}P'$ differs from that of $\bar{Q}P$, we need only consider the sequence of changes induced by the chain of transpositions that separates P' from P.

The result of a single transposition acting on P is

$$(n\ m)P = \begin{pmatrix} 1 & P1 \\ 2 & P2 \\ \vdots & \vdots \\ \bar{P}n & m \\ \vdots & \vdots \\ \bar{P}m & n \\ \vdots & \vdots \\ N & PN \end{pmatrix}. \quad \text{Hence,} \quad \bar{Q}(n\ m)P = \begin{pmatrix} 1 & \bar{Q}P1 \\ 2 & \bar{Q}P2 \\ \vdots & \vdots \\ \bar{P}n & \bar{Q}m \\ \vdots & \vdots \\ \bar{P}m & \bar{Q}n \\ \vdots & \vdots \\ N & P\bar{Q}N \end{pmatrix}. \tag{A.3}$$

As to how this differs from $\bar{Q}P$, there are three possibilities to consider. First, when $n = m$, the 2-cycle is just an identity element; the equalities $\bar{Q}P = \bar{Q}(n\ m)P$ and $\#(\bar{Q}P) = \#(\bar{Q}(n\ m)P)$ follow trivially. Otherwise, the outcome depends on whether $\bar{P}n$ and $\bar{P}m$ are in the same cycle. If they are, the transposition splits one cycle into two,

$$\bar{Q}P = (1\ 8\ 3\ \bar{P}n\ 2\ 7\ 4\ \bar{P}m\ 6\ 5)\cdots, \tag{A.4}$$

$$\bar{Q}(n\ m)P = (1\ 8\ 3\ \bar{P}m\ 6\ 5)(2\ 7\ 4\ \bar{P}n)\cdots, \tag{A.5}$$

and $\#(\bar{Q}(n\ m)P) - \#(\bar{Q}P) = +1$. If $\bar{P}n$ and $\bar{P}m$ are in different cycles, the transposition merges two cycles into one,

$$\bar{Q}P = (1\ 3\ 7\ \bar{P}n\ 4\ 6)(2\ 8\ \bar{P}m\ 5)\cdots, \tag{A.6}$$

$$\bar{Q}(n\ m)P = (1\ 3\ 7\ \bar{P}m\ 5\ 2\ 8\ \bar{P}m\ 4\ 6)\cdots, \tag{A.7}$$

and $\#(\bar{Q}(n\ m)P) - \#(\bar{Q}P) = -1$. These three cases can be summarized by

$$\#\left(\bar{Q}(n\ m)P\right) - \#(\bar{Q}P) + \delta_{n,m} = \begin{cases} +1 & \text{if } \bar{P}n \overset{\bar{Q}P}{\sim} \bar{P}m, \\ -1 & \text{otherwise} \end{cases} \tag{A.8}$$

or, equivalently,

$$\frac{\langle Q|(n\ m)P\rangle}{\langle Q|P\rangle}\left(\frac{1}{2}\right)^{1-\delta_{n,m}} = \begin{cases} 1 & \text{if } \bar{P}n \overset{\bar{Q}P}{\sim} \bar{P}m, \\ \frac{1}{4} & \text{otherwise.} \end{cases} \tag{A.9}$$

References

[1] G. Rumer, Gottingen Nachr. Tech. 1932 (1932) 377.
[2] L. Pauling, J. Chem. Phys. 280 (1933) 1.
[3] L. Hulthén, Arkiv Mat. Astron. Fys. A 26 (11) (1938).
[4] H. Bethe, Z. Phys. 71 (1931) 205.
[5] C.K. Majumdar, D.K. Ghosh, J. Math. Phys. 10 (1969) 1388.
[6] P. Fazekas, P.W. Anderson, Philos. Mag. 30 (1974) 23.
[7] P.W. Anderson, Science 235 (1987) 1196.
[8] P.W. Anderson, G. Baskaran, Z. Zou, T. Hsu, Phys. Rev. Lett. 58 (1987) 2790.
[9] S. Liang, B. Doucot, P.W. Anderson, Phys. Rev. Lett. 61 (1988) 365.
[10] M. Kohmoto, Phys. Rev. B 37 (1988) 3812.
[11] M. Havilio, A. Auerbach, Phys. Rev. Lett. 83 (1999) 4848.
[12] M. Havilio, A. Auerbach, Phys. Rev. B 62 (2000) 324.
[13] J. Lou, A.W. Sandvik, cond-mat/0605034.
[14] D. Poilblanc, Phys. Rev. B 39 (1989) 140.
[15] C. Gros, Phys. Rev. B 38 (1988) 931.
[16] L. Capriotti, F. Becca, A. Parola, S. Sorella, Phys. Rev. Lett. 87 (2001) 097201.
[17] H.Q. Lin, Phys. Rev. B 42 (1990) 6561.
[18] S. Ramasesha, Krishna Das, Phys. Rev. B 42 (1990) 10682.
[19] G.G. Balint-Kurti, M. Karplus, J. Chem. Phys. 50 (1969) 478.
[20] Z.G. Soos, S. Ramasesha, in: D.J. Klein, N. Trinajstic (Eds.), Valence Bond Theory and Chemical Structure, Elsevier, New York, 1990.
[21] F. Figueirido, et al., Phys. Rev. B 41 (1989) 4619.
[22] I. Bose, P. Mitra, Phys. Rev. B 44 (1991) 443.
[23] M. Havilio, Phys. Rev. B 54 (1996) 11929.
[24] N. Read, S. Sachdev, Phys. Rev. Lett. 62 (1989) 1694.
[25] N. Read, S. Sachdev, Phys. Rev. B 42 (1990) 4568.
[26] S.A. Kivelson, D.S. Rokhsar, J.P. Sethna, Phys. Rev. B 35 (1987) 8865.
[27] S.L. Sondhi, et al., Rev. Mod. Phys. 69 (1997) 315.
[28] S. Sachdev, Rev. Mod. Phys. 75 (2003) 913.
[29] A. Vishwanath, L. Balents, T. Senthil, Phys. Rev. B 69 (2004) 224416.
[30] T. Senthil, et al., Science 303 (2004) 1490.
[31] S. Liang, Phys. Rev. Lett. 42 (1990) 6555.
[32] G. Santoro, S. Sorella, L. Guidoni, A. Parola, E. Tosatti, Phys. Rev. Lett. 83 (1999) 3065.
[33] A.W. Sandvik, Phys. Rev. Lett. 95 (2005) 207203.
[34] O.F. Syljuåsen, et al., Phys. Rev. E 66 (2002) 046701.
[35] H.G. Evertz, Adv. Phys. 52 (2003) 1.
[36] D.S. Rokhsar, S.A. Kivelson, Phys. Rev. Lett. 61 (1988) 2376.
[37] B. Sutherland, Phys. Rev. B 37 (1988) 3786.
[38] S. Sachdev, R.N. Bhatt, Phys. Rev. B 41 (1990) 9323.
[39] Z. Nussinov, C.D. Batista, B. Normand, S.A. Trugman, cond-mat/0602528.
[40] K.S. Raman, R. Moessner, S.L. Sondhi, Phys. Rev. B 72 (2005) 064413.
[41] W. Marshall, Proc. R. Soc. London A 232 (1955) 48.
[42] B. Sutherland, Phys. Rev. B 38 (1988) 7192.
[43] M. Kohmoto, Y. Shapir, Phys. Rev. B 37 (1988) 9439.
[44] K. Binder, Z. Phys. B 43 (1981) 119.
[45] A.W. Sandvik, R.R.P. Singh, D.K. Campbell, Phys. Rev. B 56 (1997) 14510.